Crack Control for Ledges in Inverted "T" Bent Caps

Research Report 0-1854-5

Prepared for
Texas Department of Transportation
Project 0-1854

By

Ronnie Rong-Hua Zhu
Research Associate

Hemant Dhonde
Research Assistant

Thomas T.C. Hsu
Moores Professor

Department of Civil and Environmental Engineering
University of Houston
Houston, Texas

October 15, 2003

Research Report 0-1854-5

Final Report
to
Texas Department of Transportation
Project 0-1854

Crack Control for Ledges in Inverted 'T' Bent Caps

By

Ronnie Rong-Hua Zhu

Research Associate

Hemant Dhonde

Research Assistant

and

Thomas T. C. Hsu

Moores Professor

Department of Civil and Environmental Engineering

University of Houston

Houston, Texas

October 15, 2003

TxDOT Research Report 0-1854-5

Crack Control for Ledges in Inverted 'T' Bent Caps

By Ronnie R. H. Zhu, Hemant Dhonde and Thomas T. C. Hsu
Dept. of Civil & Environmental Engineering
University of Houston, Houston, TX 77204

Abstract

Inverted "T" bent caps are used extensively in concrete highway bridges because they are aesthetically pleasing and offer a practical means to increase vertical clearance. The problem is that at service load unacceptable diagonal cracks frequently occur at the re-entrant corners between the cantilever ledges and the web. In order to control the diagonal cracks, an extensive three-phase investigation was carried out. The first phase was to predict the diagonal crack widths at the interior portions of the bent caps. A 2-D analytical model, called Compatibility-Aided Strut-and-Tie Model (CASTM), was developed. This model was calibrated by the test results of seven full-size 2-D test specimens. The second phase was to predict the diagonal crack widths at the end faces of the exterior portions of bent caps. In this phase the CASTM was extended to 3-D analysis, which was calibrated by the test results of ten 3-D specimens. In the third phase, two whole-bent-cap specimens were tested to determine the effective distribution width in the vicinity of an applied load on the ledge. Crack control methods for the interior spans and the exterior end faces were recommended.

The first and second phases of research were reported in TxDOT research reports 0-1854-3 and 0-1854-4, respectively. This report (0-1854-5) serves two purposes: (1) to describe the third phase of research in details, and (2) to summarize all three phases of research.

Keywords: Bent Caps; Bridges; Crack control; Crack Width; Inverted-T Beam; Re-entrant corner; Reinforced Concrete; Serviceability.

TABLE OF CONTENTS

LIST OF TABLES

LIST OF FIGURES

Chapter 1. Introduction

1.1 Project Objectives

Inverted "T" bent caps are used extensively on Texas bridges because they are aesthetically pleasing and offer a practical means to increase vertical clearance. As shown in Fig. 1(a), the cross-section of an inverted "T" bent cap consists of a "web" with short cantilever "ledges" at the bottom to support the bridge girders, thus minimizing the structural depth of bridges. The problem is that at service load unacceptable diagonal cracking frequently occurs between the cantilever ledges and the web as shown in Fig. 1(b) and (c). In addition to giving the appearance of structural distress, excessive crack widths can lead to the corrosion of reinforcement and the shortening of service life of bridges.

At present, the design of inverted 'T' bent caps is based on ultimate strength concept (Mirza and Furlong, 1983, 1983, 1985, 1986), and is susceptible to high service-load stresses in reinforcement that cause excessive crack width. That is, the current design guidelines do not address the problem of crack control at service load adequately; thus, explicit design provisions for cracking need to be developed. The research described in this report seeks to fill this need by developing an intelligible behavioral theory that supports serviceability designs for inverted T bent caps.

The research is divided into three phases: **Phase One** deals with two-dimensional (2-D) test specimens, Fig. 1(b), that represent the interior portions of inverted T bent caps and dapped ends of bridge girders. **Phase Two** deals with three-dimensional (3-D) test specimens, Fig. 1(c), that represent the exterior portions of the bent cap where cracking is most visible. **Phase Three** deals with the bent caps as a whole, Fig. 1(d), including both the interior span and the exterior cantilever portions.

1.2 Phase One Research

Phase One Research followed a two-step methodology: First, develop a theoretical model for crack widths; and secondly, test full-size specimens and use the test results to calibrate the forces and deformations in the model to the crack widths.

The first step produces a theoretical model that not only provides a physical basis for crack widths, but also leads to a conceptually clear method of design. For the D-regions of reinforced concrete structures such as the re-entrant corners, the strut-and-tie model (Schlaich et al., 1987) is a very powerful tool for visualizing the internal flow of forces and for arranging the steel bars and concrete struts. In this type of application, only the equilibrium condition at ultimate load stage needs to be satisfied. In this research, the strut-and-tie model was applied to the prediction of crack widths by taking into account the compatibility condition at service load. This **Compatibility-Aided Strut-and-Tie Model (CASTM)** satisfies both the equilibrium of forces and the compatibility of deformations.

In the second step, in order to relate the forces of struts and ties to their deformations, and then to the crack widths, the formulation of CASTM must be accompanied by the testing of 2-D specimens as shown in Fig. 1(b). The 2-D specimens must be full-sized to avoid the similitude problems involved in reinforced concrete structures. Seven full-sized specimens were tested to calibrate the theoretical model. Since each end of a specimen supplies a set of test data, a total of

14 sets of test data is available for analysis. The calibration resulted in simple, accurate equations for predicting the diagonal crack widths at interior locations of inverted "T" bent caps and dapped ends of bridge girders.

Complete records of Phase One Research can be found in a research report TxDOT 0-1854-3 (Zhu, Wanichakorn and Hsu, 2001). A condensed version was published in a paper in the ACI Structural Journal (Zhu et al, 2003).

1.3 Phase Two Research

Phase Two Research deals with the diagonal crack widths at the exterior portion of the bent cap, Fig. 1(a). The 3-D specimen representing this region is shown in Fig. 1(c). In this region, the stresses and strains of the bent caps are three-dimensional (3-D), rather than two-dimensional (2-D) as in Phase One. Therefore, the analytical model CASTM, which applied to the 2-D specimens, was extended to 3-D specimens to predict the crack widths on the end faces.

Ten 3-D specimens were tested to study the effect of two primary variables on the crack widths of end faces. These two variables were: (1) distance from the most exterior load to the end face, and (2) the number of diagonal bars. The crack widths measured at the end faces were correlated to the CASTM model while incorporating the effect of these two variables. The proposed design formulas are reasonably simple and easy to follow.

Complete records of Phase Two research can be found in a research report TxDOT 0-1854-4 (Zhu and Hsu, 2003).

1.4 Phase Three Research

Phase Three Research deals with the tests and analyses of whole specimens. Two whole specimens were tested as shown in Fig. 1(d). The main purpose of this phase of research was to find out how far an applied service load on the ledge can distribute along the span and how many hanger bars contribute to resisting the load. This effective distribution width of hanger bars along the span is required to determine the width of a 2-D model for the calculation of the crack width. The second purpose of Phase Three Research was to check the effect of the hanger bar spacing and the size of the bearing pad on the crack width.

No separate report was issued for Phase Three research. The test specimens, test facility, and the extensive test results of the whole bent caps are described in this final report.

1.5 Scope of This Final Report

This final report summarizes the research done in phases one, two and three in chapters 2, 3, and 4, respectively. Chapter 4 contains more details of Phase Three research, because the tests of the two whole bent caps were not recorded in a separate report. In addition to describing the test facility for the whole bent caps, careful descriptions are given on the measurements of the hangar strain variation along the span and the determination of the effective distribution widths for hanger bars.

Chapter 5 summarizes the recommended design method for crack width prediction, method of crack control, and proposed code provisions. The principle of similitude is also discussed. Finally, a design example is given in Chapter 6 to illustrate the application of the proposed design method.

Chapter 2. Phase One Research: 2-D Specimens

2.1 Experimental Work

The dimensions and steel arrangement of a typical test specimen with diagonal bars (Specimen T5) are shown in Fig. 2.1(a). Because of the symmetry about its mid-span plane, each specimen can provide test data for two re-entrant corners at service load. The vertical shear reinforcement in the web of the specimen will be referred to as "hanger bars" and the horizontal flexural reinforcement in the ledge as "flexural bars". Two other types of reinforcement are "diagonal bars" oriented perpendicular to the diagonal crack and "shear-friction bars" placed horizontally at the mid-depth of ledges (flanges). Specimen T5 in Fig. 2.1(a) contains diagonal bars, but no shear-friction bars.

In order to study the effectiveness of these four types of reinforcement, different proportions of steel were provided in the seven specimens as shown in Table 2.1. The service load capacities of these seven specimens are given. The ultimate load capacities are also given, except that of specimen BPC1. This special specimen was tested with a different objective in mind (studying a repair method using carbon fiber sheets).

Service load is difficult to define because the yielding sequences of hanger, flexural and diagonal bars vary for reinforcing steel arrangements. For convenience, service load is defined as a range from 60% of the first bar yield load to 60% of the last yield load.

4000 psi ready-mix concrete and Grade 60 deformed No. 6 steel bars with average yield strength of 64,000 psi (441 MPa) were used for all specimens.

A total of 38 linear voltage displacement transducers (LVDTs) and 24 SR4 electrical strain gauges were used to instrument each specimen. The average strains of concrete and steel bars were measured by 14 LVDTs on each side of a specimen. Eleven LVDTs were arranged in a pattern according to the proposed strut-and-tie model and in such a way that the strain data could be cross-checked (Fig. 2.1(b)). At three locations along the diagonal cracks, LVDTs were installed to measure the diagonal crack widths over a gauge length of 9.5 in. (241 mm).

Hand-held microscopes were also used to measure widths of the diagonal cracks at the re-entrant corners of the specimens.

2.2 Crack Width Prediction Using CASTM

The CASTM (Compatibility-Aided Strut-and-Tie Model) without diagonal bars is shown in Fig. 2.2(a). This truss model is statically determinate so that the forces in the hanger bars H and in the flexural bars F can be calculated directly from the applied loads V on the ledges. These forces H and F are converted into strains ε_H and ε_F, respectively, using their axial stiffness. These strains are used to form the diagonal crack strain $\varepsilon_{HF} = \sqrt{\varepsilon_H^2 + \varepsilon_F^2}$. Multiplying ε_{HF} by a CASTM gauge length L_{HF} results in the diagonal crack width w at the re-entrant corners. This CASTM gauge length L_{HF} was calibrated by the tests of full-size 2-D specimens to be $L_{HF} = 9500\,\varepsilon_{HF} - 3.0$ (in.).

The CASTM model with diagonal bars is shown in Fig. 2.2(b). This truss model is statically indeterminate, but can be decomposed into two statically determinate sub-trusses, one consists of hanger bars and flexural bars while the other is made of diagonal bars. When a load

2V is applied at midspan, these two sub-trusses must deflect the same amount at this point. This deformation compatibility condition is used to determine the distribution factor B for diagonal bars. The sub-truss with diagonal bars should resist a load of BV at each ledge, while the sub-truss with hanger bars and flexural bars must resist a load of (1-B)V at each ledge. Using extensive virtual work analysis, the distribution factor was calculated and then simplified to be B $= \dfrac{A_{SD}}{A_{SH} + 0.5A_{SF} + A_{SD}}$.

The CASTM model *with* or *without* diagonal bars was verified by the tests of seven full-size 2-D specimens. The design equations of CASTM *with* diagonal bars are identical to those *without* diagonal bars, except that the former involves the distribution factor B. When B is taken as zero, the CASTM *with* diagonal bars simplifies to the CASTM *without* diagonal bars.

The diagonal crack widths w at the re-entrant corners of inverted T bent caps *with or without* diagonal bars can be predicted by CASTM as follows:

$$w = L_{HF}\varepsilon_{HF} \tag{2.1}$$

where

w = predicted diagonal crack width (in.)

L_{HF} = CASTM gauge length for calculated hanger and flexural steel strains $= 9500\,\varepsilon_{HF} - 3.0$ (in.)

ε_{HF} = diagonal crack strain calculated by hanger and flexural strains $= \sqrt{\varepsilon_H^2 + \varepsilon_F^2}$

ε_H = hanger strain or strain in the vertical direction $= \dfrac{(1-B)V}{1.2E_S A_{SH}}$

ε_F = flexural strain or strain in the horizontal direction $= \dfrac{(1-B)V\cot\theta_V}{1.2E_S A_{SF}}$

V = applied service load at each ledge (in kips)

θ_V = angle between flexural steel bars and the diagonal strut at the point of load V

B = distribution factor for diagonal bars $= \dfrac{A_{SD}}{A_{SH} + 0.5A_{SF} + A_{SD}}$

A_{SD} = total cross-sectional area of diagonal reinforcement at each ledge of 2-D specimen (in.^{2})

A_{SH} = total cross-sectional area of hangar reinforcement at each ledge of 2-D specimen (in.^{2})

A_{SF} = total cross-sectional area of flexural reinforcement at each ledge of 2-D specimen (in.^{2})

E_S = 29,000 ksi

It should be noted that a simplification has been made in the above derivation, as compared to previous reports (Zhu, Wanichakorn, and Hsu, 2001; Zhu, Wanichakorn, Hsu and Vogel, 2003), in which the stiffness of a steel tie surrounded by concrete cover was calculated by $EA = E_S A_S + E_C A_C$. In this expression, E_C is the tensile modulus of elasticity of concrete given

as $E_C(\text{ksi}) = 1.87\sqrt{f'_C(\text{psi})}$, not the compressive modulus of elasticity given as $E_C(\text{ksi}) = 57\sqrt{f'_C(\text{psi})}$. A_C is the area of concrete surrounding the steel tie. In this simplification, we assume that $E_C A_C = 0.2 E_S A_S$, resulting in $EA = 1.2 E_S A_S$ (see Appendix A). This simplified stiffness of steel tie is used in the above calculation of hanger steel strain ε_H and the flexural steel strain ε_F.

2.3 Comparison of CASTM with Tests

The predicted results based on recommended design equation (2.1) are compared to the crack widths measured by LVDTs as shown in Figure 2.3(a). It can be seen that the CASTM predictions match the test results very well, particularly in the service load range. Table 2.3 compares the CASTM predictions with the test results at the mid-point of the service load range. Two test data points, one from each end of a specimen, are compared to the predicted crack widths in Figure 2.3(b). It can be concluded that the predictions are well supported by the test results.

Chapter 3. Phase Two Research: 3-D Specimens

3.1 Experimental Work

Ten 3-D specimens are listed in Table 3.1. Two primary variables were investigated; (1) the load position from the most exterior load to the end face, and (2) the number of diagonal bars. The spacing of hanger bars, flexural bars and diagonal bars are maintained at a constant of 4 in. center-to-center.

The 3-D test specimens as shown in Fig. 3.1(a) and (b) are symmetrical about the vertical centerlines of the end face, so that each end face can furnish two diagonal crack widths, one on the west side and one on the east side. Figure 3.1(c) shows the steel cage without diagonal bars and Figure 3.1(d) shows the steel cage with diagonal bars.

The concrete used in the 3-D specimens of Phase Two study was the same as that used in the 2-D specimens of Phase One study. Grade 60 No. 5 rebar was used for the hanger and flexural bars. The average yield stress was 64.0 ksi, and the yield strain was 0.0022.

The nominal shear resistance V_n for the service limit state is calculated based on the following equation according to AASHTO Standard Specifications for Highway Bridges Eq. (5.13.2.5.5-1) (AASHTO, 2000):

$$V_n = \frac{A_{hr}(0.5f_y)}{S}(W + 3a_v) \qquad (3.1)$$

where
- V_n = the nominal shear resistance, in kips, for single-beam ledges
- A_{hr} = area of one leg of hanger reinforcement (in^2)
- S = spacing of hangers (in)
- f_y = yield strength of reinforcing steel (ksi)
- W = width of bearing (in)

a_v = distance from face of wall to the load (in)

Eq. (3.1) does not take into account the cases where $W + 3a_v$ is larger than the spacing of the bearings or is larger than 2 times the distance L_E from the center of bearing pad to the end face. In the case of exterior bearing pad and $W + 3a_v > 2L_E$, the following equation should apply:

$$V_n = \frac{A_{hr}(0.5f_y)}{S} 2L_E \tag{3.2}$$

The nominal shear resistance V_n for the service limit state calculated for the ten 3-D specimens are given in Table 3.1.

All specimens were tested in the 2.5-million lbs MTS testing system, located at the University of Houston Structural Research Laboratory. The test set-up is shown in Fig. 3.1(a) and (b).

As shown in Fig. 3.1(b) the load V was calculated from the applied load P by the following formula:

$$V = \frac{P}{2}\left(\frac{13 \text{ in.}}{67 \text{ in.} - L_E}\right) \tag{3.3}$$

When L_E = 10 in., V = 0.114 P.

This MTS test system is controlled by a versatile TestStar system, which can provide both load-control and strain-control procedures. The load was first applied by the load-control procedure in the linear stage of load-deformation curve, and was then switched to the strain-control mode when the curve became non-linear. A continuous record of the stresses and strains was obtained during the test.

A total of 35 LVDTs and 40 SR4 electrical strain gauges were available to test each specimen. They were placed at the most desirable locations to maximize the required information according to the design of each specimen. For most of the specimens, the strains of concrete and steel on the end face of a specimen were measured by 16 LVDTs. For specimens used to study the variation of strains in hanger bars along the span direction, the hanger strains were measured by 14 LVDTs as shown in Fig. 3.1(e).

3.2 Design Equations for Crack Width Control

The model for predicting crack widths at re-entrant corners of 3-D specimens was developed based on the CASTM for 2-D specimens. The first curtain of exterior hanger bars, flexural bars and diagonal bars are treated as a 2-D truss. The steel area of the first curtain of exterior hanger bars, flexural bars and diagonal bars are used to calculate the diagonal crack width as follows:

$$w = \frac{1.8L_{HF}\varepsilon_{HF}}{(1+L_E)^2} \le 0.004 \text{ in.} \tag{3.4}$$

$$w = \frac{0.18(1-B)^5(V - V_{0.004})}{(1+L_E)^2} + 0.004 \text{ in.} \le 0.015 \text{ in.} \tag{3.5}$$

where

w = predicted diagonal crack width (in.)

L_{HF} = CASTM gauge length for calculated hanger and flexural steel strains
= $9500\varepsilon_{HF}$ - 3.0 (in.)

L_E = distance from end face to the service load V applied on the exterior bearing pad.

ε_{HF} = diagonal crack strain calculated by hanger and flexural strains
= $\sqrt{\varepsilon_H^2 + \varepsilon_F^2}$

ε_H = hanger strain or strain in the vertical direction = $\dfrac{(1-B)V}{1.2E_S A_{SH}}$

ε_F = flexural strain or strain in the horizontal direction = $\dfrac{(1-B)V\cot\theta_V}{1.2E_S A_{SF}}$

V = applied service load at an exterior loading pad (kips)

θ_V = Angle between flexural steel bars and the diagonal strut at the point of load V

B = distribution factor for diagonal bars = $\dfrac{A_{SD}}{A_{SH}+0.5A_{SF}+A_{SD}}\left(\dfrac{0.44NS_D}{1+L_E}\right)$

A_{SD} = cross-sectional area of a diagonal steel bar at end face of inverted 'T' bent cap(in.^{2})

A_{SH} = cross-sectional area of a hangar steel bar at end face of inverted 'T' bent cap(in.^{2})

A_{SF} = cross-sectional area of a flexural steel bar at end face of inverted 'T' bent cap(in.^{2})

N = number of diagonal bars from the end face to the center of first bearing.

S_D = center-to-center spacing of diagonal bars, same as spacing of hangar bars.

E_S = 29,000 ksi.

$V_{0.004}$ = applied service load V (kips) at exterior bearing pad corresponding to a crack width of 0.004 in. $V_{0.004}$ can be calculated from Eq. (3.4) using a successive approximation method easily performed on a spreadsheet.

It should be noted that L_E (distance from the exterior load to the end face) has been used in Eqs. (3-4) and (3-5) to replace L_V (distance from the exterior load to the most exterior bar) used in the research report TxDOT 0-1854-4 (Zhu and Hsu, 2003). Accordingly, the power of 1.9 in the denominator becomes 2 and a constant 1.8 is inserted in the numerator. This change makes it much easier and more convenient to use Eq. (3.4) and (3.5). Also, the expression for the distribution factor B has also been simplified.

3.3 Comparison with Tests

Figure 3.3 shows that the predicted results match the test results well, except for specimen E-0-14. This figure also shows that the predicted values are usually larger than the test values when the crack width w is less than 0.004 inch. This is because a constant concrete stiffness for cracked concrete is used for the whole process. If a varied concrete stiffness were used, the prediction would be more precise. However, the use of varied concrete stiffness would be too complicated for practical design. For the purpose of controlling crack width under 0.007

inch, a limit recommended by ACI Committee 224 (2001) for exposure to deicing chemicals, the prediction of the crack widths between 0.004 in. and 0.007 in. is useful.

Table 3.3 compares the test values and the predicted values of the loads $V_{0.004}$ and $V_{0.007}$, corresponding to crack widths of 0.004 in. and 0.007 in. For most specimens, the force differences between test results and predictions are about 5%. In short, the crack widths should be comfortably less than 0.004 in., when the service loads are limited to $V_{0.004}$.

3.4 Characteristics of Diagonal Crack Development

Fig. 3.3 clearly shows a remarkable characteristic of diagonal crack development at the end face of 3-D specimens. The diagonal crack width versus load V curve exhibits two very distinctive load stages. When the crack width is less than 0.004 in., the crack development is slow and the slope of the curve is small. Beyond a value of 0.004 in., however, crack width increases rapidly and the curve exhibits a large slope.

This difference in cracking behavior before 0.004 in. and after 0.004 in. can be explained by the two photographs of specimen E-1-10 shown in Fig. 3.4(a) and (b). Fig. 3.4(a) shows the crack pattern at P = 425 kips when w is less than 0.004 in. and Fig. 3.4(b) shows the crack pattern at P = 435 kips (a 10 kips increase) when w is larger than 0.004. When w reaches about 0.004 in., the horizontal cracks became connected and a new mechanism of resistance arises. In this post-0.004 in. stage, the concrete stiffness reduces dramatically and the stresses in the steel bars increase rapidly. In short, the value of 0.004 in. is a "critical crack width" that should not be exceeded.

This observed characteristic of diagonal crack development at end faces of bent caps leads us to a sensible criterion for crack control. Instead of checking a crack width at service limit state and comparing it to a specified value, we can simply calculate the force that will produce a critical crack width and compare it to the load designed for service limit state.

Chapter 4. Phase Three Research: Whole Bent Caps

4.1 Objectives and Scope

Phase Three research deals with both the interior portion and the exterior cantilever portions of an inverted T bent cap. In the interior portion, the primary purpose is to predict the maximum crack width in the vicinity of a load V acting on the ledge. To do so, we can isolate a slice of the interior portion (a 2-D specimen) that contains the load V as shown in Fig. 1(a). The width of this 2-D specimen (studied in Chapter 2) will be called the effective distribution width, L_D. This width L_D is determined by measuring the strains of hanger bars along the span on both sides of the load V. Dividing the load V by the total steel area of hanger bars in the width L_D will give the maximum hanger stress for the calculation of the maximum crack width.

The exterior cantilever portions of a whole bent cap have been simulated by the 3-D specimens discussed in Chapter 3. Equations for crack width prediction were derived from these tests. Therefore, the testing of whole bent caps can serve two additional purposes: (1) to check the recommended equations derived from the 3-D test specimens, and (2) to check the effect of spacing of hanger bars and number of diagonal bars on the crack width.

4.2 Experimental Work

4.2.1 Test Specimens

Two 20-feet long specimens W1 and W2, as shown in Fig. 4.2.1, were tested. Labels N and S represent the north and south ends, respectively, of the whole specimen. Labels A, B, C and D denote the location of the four actuators. The hanger bars under Actuators B and C are loaded to obtain the effective distribution width L_D along the span.

Table 4.2 shows the variables in the tests. First, the two variables affecting the width L_D are the bearing pad width and the spacing of hangar bars in the interior span. Second, the number of diagonal bars and the spacing of hanger bars are the variables in the study of crack widths in the exterior portions.

The same concrete was used in all three phases of research. The concrete was Class F, six-sack, ready-mix, and had a compressive strength of 4700 psi or more. The hanger and flexural bars were made of No. 5 reinforcing bars of Grade 60. The average yield stress of the steel bars was 64.0 ksi, and the yield strain was 0.0022.

4.2.2 Loading Method

The test specimen was installed in the test frame as shown in the photos of Fig. 4.2.2(a) and (b). The test frame was specially designed to have a working capacity of 1050 kips, and was located in the Structural Research Laboratory at the University of Houston. Four MTS hydraulic actuators, A, B, C and D, of 223, 340, 340 and 147-kip capacity, respectively, were used to apply loads on the bent cap. These four loads ensure pure bending between frames B and C, thus guaranteeing an unbiased failure zone.

The actuators were controlled by a versatile FlexTestGT system that allowed load-control as well as strain-control procedures. This system has a Multipurpose Test (MPT) feature that allows the four actuators to work independently or in unison under either a force-control or a displacement-control mode. Moreover, this system offered a unique feature to “hold” (or maintain constant) the forces or the displacements of the actuators. Loading was first applied by the load-control procedure in the linear stage of the load-deformation curve. When the load-deformation curve became non-linear, the loading was switched to the strain control mode.

Initially, the four actuators applied equal loads at the rate of 20 lbs/sec, until actuator D reached its capacity of 147 kips. In the second stage, actuators A and D were kept on “hold” at 147 kips force, while the forces in actuators B and C were increased until failure in the interior span. In the third stage, the actuators B, C and D were on “hold”, while the force in actuator A was increased until failure occurred at the north end. In the last stage of the test, the specimen was rotated 180 degree and reinstalled to test its south end using actuator A until failure.

4.2.3 Test Frame

The test frame is depicted in a series of Figures 4.2.3(a) to (d). Fig. 4.2.3(a) shows the horizontal plan view of the test frame, consisting of two longitudinal beams (anchored to the strong floor) on which are mounted the four vertical frames: A, B, C and D. Each vertical frame is equipped with a corresponding actuator with the same label, Figs. 4.2.3(b) to (d). Frame A, along with its bottom anchoring beam, was designed to be detachable and movable, thus allowing easy installation and removal of a 20-ft specimen.

The inverted-T cap is supported on the bottom by two reaction load cells of 500 kips capacity each. Each load cell sits on an assembly of a rod sandwiched between two plates, on top

of a pedestal. Pedestal 1 offers a hinged support while Pedestal 2 serves as a roller support. The roller support allows free longitudinal movement of the test specimen.

Actuators B, C and D are each provided with a swivel base at the top end and one at the bottom end, allowing for compensation of eccentricities, rotation and movements of the test specimen. Actuator A serves to anchor the test specimen in space and is, therefore, not provided with swivel bases at both ends. The force exerted by each actuator is split equally to the west and east ledges of the test specimen by the Π-shaped steel rig. Each of the two legs of the steel rig sits on the ledge through a high-strength steel ball and a bearing plate. Bearing plates of sizes 6 x 6 x 1.25 inch were used for frame A, C & D, while 10 x 6 x 1.25 inch plates were used for frame B.

The three actuators, B, C and D, are each equipped with a spherical hinge at the lower end, allowing the Π-shaped steel rigs to pivot. In order to prevent the lateral buckling of an actuator at this location, a lateral bracing system is provided, which consists of a pair of channel beams spanning between the two frame columns at the level of the spherical hinge.

4.2.4 Instrumentation

A total of 35 LVDTs and 40 SR4 electrical strain gauges were available for testing each specimen. The instruments were placed at the most desirable locations to maximize the required information according to the design of each specimen. The strains on each end face along the steel bars and perpendicular to a diagonal crack were measured by 6 LVDTs as shown in Fig. 4.2.4(a) and (b).

In order to study the variation of strains in hanger bars along the span direction, 23 LVDTs were installed to measure the hanger bar strains as shown in Fig. 4.2.4(c) and (d). Before casting concrete, two short threaded rods were first welded to a vertical leg of the hanger bar, one near the top corner and the other near the bottom corner. After casting the concrete, the upper threaded rod protruded from the vertical surface of the web and received an aluminum bracket. The lower threaded rod, which protruded from the bottom surface of web, also received an aluminum bracket that clamps an LVDT. The LVDT, which is under the ledge, is attached to the upper bracket via a vertical aluminum rod passing through a plastic-tube-lined hole in the ledge. In this manner, the LVDT measured the vertical displacement between the two aluminum brackets, thus giving the average strain of a hanger bar.

4.3 Test Results

4.3.1 Crack Width Control

Figure 4.3.1(a) compares the crack widths at C2 (see Fig. 4.2.4(b)) measured by microscopes (MS) and by LVDTs. The labels NE, NW, SE and SW in these graphs represent the locations of the instruments. The first letter, N and S, indicates the north and south end faces. The second letter, E and W, indicates the east and west sides on the end faces. Crack widths measured by these two different methods match well overall. However, the crack widths on the west side and on the east side measured by microscopes show some differences, while they should theoretically be the same.

Figure 4.3.1(b) shows the effect of two variables on crack widths measured by LVDTs, namely, the number of diagonal bars and the spacing of hanger bars. Each exterior cantilever span of a whole specimen is assigned a label according to the labeling convention for 3-D specimens (see Table 3.1, first column). For example, (E-2-14, s = 4) means that the 3-D

specimen has two diagonal bars and the distance from the outer-most load to the end face is 14 in. And, the spacing of the hanger bars s is 4 in.

Fig. 4.3.1(b) compares the test results from Specimens W1-NE (E-2-14, s=4) and Specimen W1-SW (E-4-14, s=4). It can be seen that under the same conditions, a specimen with 4 diagonal bars achieved better crack width control than a specimen with 2 diagonal bars.

Fig. 4.3.1(c) compares the test results obtained from the LVDTs at C2 with the prediction based on equations proposed for 3-D specimens (Phase Two research). It can be seen that the actual test results match the theoretical prediction satisfactory, except for specimen W1-NE (E-2-14, s=4). In this case, there was a discrepancy when the crack width was larger than 0.004 in., but was acceptable when crack width was less than 0.004 in.

4.3.2 Hanger Strain Variation Along Span

Hanger strain variations measured in specimen W1 and W2 are shown in Fig. 4.3.2(a) to (d). The horizontal axis represents the distance of a hanger bar from the center of bearing pad. The line at 0 distance represents the center of bearing pad, and the positive distance means that a hanger bar is in the pure bending region; while the negative distance means that a hanger is in the shear-flexure region. The two dash vertical lines represent the two edges of the bearing pad. Fig. 4.3.2(a) to (d) shows that when load V is around 70 kips, the hanger strains begin to increase very quickly, signifying a rapid opening of diagonal cracks.

In order to study the effect of bearing pad width on the strain variations, the hanger strain variations along the B and C regions are plotted together in Figures 4.3.2(e) and (f). The bearing pad width for Actuator B and C is 10 in. and 6 in., respectively. It can be seen that the bearing pad width does have an effect on the distribution of hanger bar strains along the span. The distribution of strains was more spread out in the B region than in the C region. This is particularly true in Figure 4.3.2(f) where the two hanger bars just outside the bearing pad for W2-C show roughly the same or even larger strains than the two bars under the bearing pad. Overall, the evidence shows a direct relationship: the larger the loading pad width, the larger the effective distribution width along span.

Figures 4.3.2(g) and 4.3.2(h) illustrate the effect of hanger bar spacing on the hanger strain variation. The hanger spacing for W1 and W2 is 4 in. and 5.5 in., respectively. It can be seen that the hanger spacing has no discernable effect on the distribution of hanger bar strains along the span, and, therefore, should have no effect on the effective distribution width of hanger bars.

4.3.3 Effective Distribution Width of Hanger Bars

The effective distribution width can be determined experimentally using the measured strain variation along the span. Fig. 4.3.2(a) to (d) show that the hanger strain variation is distributed like a bell-shaped curve. The strain of hanger bars within the width of bearing pad is generally larger than the strain of hanger bars outside the width of bearing pad. The average value of the hanger bar strains within the bearing pad width is used in calculating the crack width. Since the hanger strain variations in the pure flexure region between B and C is different from those in the shear-flexure regions between A and B or C and D, only the hanger strains in pure bending regions have been used.

Assuming that the effective distribution width L_D is a function of the bearing pad width W and the effective depth of ledge d_e:

$$L_D = W + x\, d_e \qquad (4.1)$$

where x is a coefficient to be determined by tests.

Summing the hanger bar forces in the pure flexure region, the distribution width L_D can be determined by the following equation:

$$L_D = \frac{2\sum_{i=1}^{N} F_i}{\frac{F_N}{S}} \tag{4.2}$$

where

N = number of hanger bars in pure flexure region between B and C

F_i = hanger bar force in ith bar, kips (see Fig. 4.2.1)

F_N = average force of two hanger bars within the pad width such as B7 and B8 of W1, kips. The average value of two hanger bars is used to get a more stable result.

S = hanger bar spacing.

The coefficient x can be obtained by equating Eq. (4.1) with (4.2) as shown in Tables 4.3.3(a) to (c). The first two rows in each table are the loading stages in which the hanger bar strains begin to jump or increase rapidly. The distribution width obtained in those two loading stages should be used to predict crack width at service load. The distribution width of W2-C given in Table 4.3.3(d) was not taken into account, because concrete was not well compacted during casting in this region.

The results from Table 4.3.3(a) to (c) show that the effective distribution width is not a function of hanger spacing. At service load stage, the distribution width can be taken as $W + 0.9d_e$. At the ultimate load stage, however, the distribution width can be taken as $W + 1.8d_e$.

4.3.4 Diagonal Crack Width Prediction at End Faces

One of the purposes for testing the whole pile caps was to check the validity of Eqs. (3-4) and (3-5) derived from testing 3-D specimens. Fig. 4.3.1(c) compares the measured values to the predicted values of diagonal crack widths at the end faces of whole specimens. It can be seen that Eqs. (3-4) and (3-5) can be applied to the whole specimen without modification. The agreement also means that the test set-up and the test method for 3D specimens, as shown in Fig. 3.1(a) and (b), is validated.

It should be noted that Eqs. (3-4) and (3-5) do not include the hanger bar spacing as a variable. However, the hanger bar spacing is different in each of the four end cantilever spans of the two specimens, W1 and W2. This agreement between the experimentally measured and the predicted crack widths in Fig. 4.3.1(c) proves that the hanger bar spacing is in fact not a variable in the crack prediction and can be excluded from consideration. In general, such simplified equations can very well predict the important load $V_{0.004}$ at the critical crack width of 0.004 in. at the end faces of inverted T beams. This is a significant step towards more clarity in crack prediction.

4.4 Similitude Requirements

Eq. (3.4) is valid for inverted T-beam of the size tested in this research and can produce the correct value of 0.004 in. for the critical crack width. However, Eq. (3.4) is not expected to be valid when applied to the full-size bent caps, because a scaling ratio must be incorporated. This scaling ratio can be derived from the principle of similitude.

When a prototype structure is the object of investigation, numerical or physical modeling is usually taken. The knowledge and experience gained by working with small-scale models are important. Muller (1992) pointed out that "the actual behavior of a reinforced concrete structure with regard to cracking loads and failure is very strongly influenced by the bond between concrete and reinforcement, and this cannot be reproduced by numerical models, not even by very elaborate ones." Therefore, the scale of a test model should be as large as possible to prevent introducing unpredictable scale effects. But practical laboratory constraints will limit the test model size.

For this research project, experimental specimens were designed as large as possible. No. 5 steel bars were used in the ten 3-D specimens and in the two whole test specimens to provide the best bond similarity with the No. 6 bars used in full-size bent caps. The scale ratios of the test specimens and the full-size bent caps are shown in Table 4.4(a). The theory involved in the relationship between physical quantities was given by Gibson (1992) and summarized in Table 4.4(b). A listing of quantities, their dimensions and scaling factors are given in Table 4.4(c), where the independent scaling factors chosen are the modulus of elasticity S_E and the length S_ℓ.

In reinforced concrete structures, the scaling ratios for modulus of elasticity and stress S_E can be taken as unity. The scaling ratios for length S_ℓ can be taken as the root average of the three scaling ratios for lengths that are crucial in determining the strength and cracking of the bent caps: (1) the height measured from the centroid of bottom flexural bar to the centroid of top flexural bar ($d_d - c - 0.5d_b$), (2) the distance from the load V to the center of hanger bar (a_f), and (3) the area of hanger steel bar (A_{SH}). The average scaling ratio is calculated as follows:

$$S = S_\ell = \left[\frac{(d_e - c - 0.5d_b)_p (a_f)_p (A_{SH})_p}{(d_e - c - 0.5d_b)_m (a_f)_m (A_{SH})_m} \right]^{\frac{1}{4}} \tag{4.3}$$

$$= \left[\frac{11.9 \times 16.25 \times 0.44}{7.25 \times 9 \times 0.31} \right]^{\frac{1}{4}} = 1.43$$

where the subscript p means prototype and the subscript m indicates model.

Eqs. (3.4) and (3.5) obtained from the model tests are converted to equations for the prototype structure based on scaling factor as follows:

$$w = \frac{S(1.8 L_{HF} \varepsilon_{HF})}{(1 + \frac{L_E}{S})^2} \le S(0.004 \text{ in.}) \tag{4.4}$$

$$w = \frac{S(0.18)(1 - B)^5 (\frac{V}{S^2} - \frac{V_{0.006}}{S^2})}{(1 + \frac{L_E}{S})^2} + S(0.004) \text{ in.} \tag{4.5}$$

Substituting S = 1.43 into Eqs. (4.4) and (4.5) gives:

$$w = \frac{2.6 L_{HF} \varepsilon_{HF}}{(1 + 0.7 L_E)^2} \le 0.0057 \approx 0.006 \text{ in.} \quad w \le 0.006 \text{in.} \tag{4.6}$$

$$w = \frac{0.13(1 - B)^5 (V - V_{0.006})}{(1 + 0.7 L_E)^2} + 0.006 \text{ in.} \qquad w > 0.006 \text{in.} \tag{4.7}$$

Appendix B gives a simplified equation to calculate $V_{0.006}$ from Eq. (4.6) for use in Eq. (4.7).

To verify the applicability of Eqs. (4.6) and (4.7) considering similitude requirement, the crack widths at re-entrant corners of inverted "T" bent caps in the bridge at Laura Koppe road, Houston, were measured as shown in Fig. 4.4(a) and (b). The input data and the predicted results are shown in Table 4.4(d). It can be seen from the table that the calculated crack width considering similitude requirements matches the measured crack width surprisingly well.

It is interesting to mention that Eqs. (4.6) and (4.7) with similitude consideration were derived prior to the measurements of crack widths in the bridge at Laura Koppe Road. Since Eq. (4.7) gave unexpected large crack widths, an arrangement was made with TxDOT to measure the crack width on-site. It was very satisfying to find that the measured crack widths matched the predictions so well.

Chapter 5. Recommended Design Method

5.1 Crack Control

5.1.1 Vicinity of Interior Applied Load

Crack control at the vicinity of interior applied load can be achieved by limiting the crack width to 0.013 in. (ACI 318, 1995). An interior applied load could act on the interior span or on an exterior portion. Diagonal crack widths are calculated directly from Eq. (2.1) based on the CASTM model for 2-D specimens. The width of the 2-D specimens is the effective distribution width L_D, given by $L_D = W + 0.9 d_e$.

Eq. (2.1) shows that adding diagonal bars is an effective way to control crack widths at the vicinity of the interior applied loads.

5.1.2 End Face of Exterior Portion

To control diagonal crack widths at the end faces, it is very important to limit the service load to a "critical load" where crack widths begin to widen rapidly. As specimen W1 (E-4-14) in Fig. 5.1 shows, when the crack width reaches about 0.004 inch, cracks opened up very rapidly even with a very small increase of load. Even though the load $V_{0.004}$ was held constant at 74 kips for four hours, the crack width continued to open up until reaching a value beyond 0.007 in.

In short, crack control at the end face of exterior span is to keep the load within the "critical load". For the inverted T beams W1 and W2, the critical crack width was 0.004 in. and the critical load was $V_{0.004}$. The critical load can be calculated from Eq. (3.4) using a spread sheet and a trial and error method.

It should be noted from Eq. (3.4) that the most effective variable to control crack width at the end faces of cantilever portions is L_E, the distance from end face to the most exterior load. Adding diagonal bars was found to be not very effective.

5.2 Proposed Code Provisions for AASHTO Specifications

5.13.2.5.7 Serviceability Limit States Design

Using the notation in Figure 1 (Fig. 5.2 in this report), the crack widths in inverted T-beam shall not be larger than:

- For Vicinity of Interior Applied Load

$$w = L_{HF}\varepsilon_{HF} \le 0.013 \text{ in} \qquad (5.13.2.5.7\text{-}1)$$

where:

w = predicted diagonal crack width (in.)

L_{HF} = CASTM gauge length for calculated hanger and flexural steel strains

= $9500\,\varepsilon_{HF}$ - 3.0 (in.)

ε_{HF} = diagonal crack strain calculated by hanger and flexural strains

= $\sqrt{\varepsilon_H^2 + \varepsilon_F^2}$

ε_H = hanger strain or strain in the vertical direction = $\dfrac{(1-B)V}{1.2E_S A_{SH}}$

ε_F = flexural strain or strain in the horizontal direction = $\dfrac{(1-B)V\cot\theta_V}{1.2E_S A_{SF}}$

V = applied service load at the most exterior loading pad (kips)

θ_V = Angle between flexural steel bars and the diagonal strut at the point of load V

B = distribution factor for diagonal bars = $\dfrac{A_{SD}}{A_{SH} + 0.5A_{SF} + A_{SD}}$

A_{SD} = total cross-sectional area of diagonal reinforcement in the effective distribution width L_D (in.^{2})

A_{SH} = total cross-sectional area of hangar reinforcement in the effective distribution width L_D (in.^{2})

A_{SF} = total cross-sectional area of flexural reinforcement in the effective distribution width L_D (in.^{2})

L_D = $W + 0.9d_e$ (in.)

W = width of bearing pad (in.)

d_e = effective depth of ledge from extreme compression fiber to centroid of tensile force (in)

E_S = 29,000 ksi

- For End Face of Exterior Portion

$$w = \frac{2.6 L_{HF} \varepsilon_{HF}}{(1 + 0.7 L_E)^2} \le 0.006 \text{ in.} \qquad (5.13.2.5.7\text{-}2)$$

where:

B = distribution factor for diagonal bars $= \dfrac{A_{SD}}{A_{SH} + 0.5A_{SF} + A_{SD}} \left(\dfrac{0.44 N S_D}{1 + L_E} \right)$

A_{SD} = cross-sectional area of a diagonal steel bar at end face of inverted 'T' bent cap ($in.^2$)

A_{SH} = cross-sectional area of a hangar steel bar at end face of inverted 'T' bent cap ($in.^2$)

A_{SF} = cross-sectional area of a flexural steel bar at end face of inverted 'T' bent cap ($in.^2$)

L_E = the distance from end face to the load V applied on the most exterior bearing, inch.

N = number of diagonal bars from the end face to the center of first bearing.

S_D = center-to-center spacing of diagonal bars, same as spacing of hangar bars.

Chapter 6. Design Example

The proposed code provisions are used to check an existing inverted T-beam in the Spring Cypress Overpass designed by TxDOT in April, 1999. Figure 6.1 shows an interior span of an inverted T-beam and an exterior cantilever portion with normal (perpendicular) end face. Figures 6.2 to 6.4 show a cantilever span of the inverted T-beam with skew end face and its steel arrangement. Figure 6.5 shows a section parallel to the skew end face.

Calculation for the cantilever portion is made by solving Eq. (5.13.2.5.7-2) to find $V_{0.006}$. The trial and error procedure is done by a spreadsheet program Excel as shown in Figure 6.6. The contents in Excel is divided into three parts: (1) input data, (2) calculation done by Excel, and (3) calculated output results.

(1) Input Data

The input data includes:

V = design service load

θ = skew angle of end face

c = clear concrete cover

h = ledge height

a_V = normal distance from load V to web edge

L_E = distance from load V to end face

d_{bH} = hanger bar diameter

A_{SH} = hanger bar area in a bar or in a bundle

d_{bF} = flexural bar diameter

A_{SF} = flexural bar area in a bar or in a bundle

A_{SD} = diagonal bar area in a bar

N = number of diagonal bar in distance L_E

S_D = diagonal bar spacing (should be equal to hanger bar spacing)

E_S = modulus of elasticity of steel reinforcement

(2) Calculations done by Excel

After all required data have been input, a trial and error method will be used to find $V_{0.006}$ using the Excel program:

Assume a value of $V_{0.006}$ = 135.5 kips

$$a_f = \frac{a_v + c}{\cos\theta} + 0.5d_{bH} = \frac{9.5 + 2.0}{\cos 0^\circ} + 0.5(0.75) = 11.875 \text{ in}$$

$$\theta_v = \arctan\frac{h - 2c - d_{bF}}{a_f} = \arctan\frac{21 - 2(2.0) - 0.75}{11.87} = 53.85^\circ$$

Since $A_{SD} = 0$

A_{SH} = 0.44 in.^{2}

A_{SF} = 0.44 in.^{2}

L_E = 29.9 in.

S_D = 4.08 in.

$$B = \frac{A_{SD}}{A_{SH} + 0.5A_{SF} + A_{SD}}\left(\frac{0.44NS_D}{1 + L_E}\right)$$

$$= \frac{0}{0.44 + 0.5(0.44) + 0}\left(\frac{0.44(0)(4.08)}{1 + 29.9}\right) = 0$$

$$\varepsilon_H = \frac{(1 - B)V}{1.2E_S A_{SH}} = \frac{(1 - 0)\,135.5}{1.2(29{,}000)(0.44)} = 0.008849$$

$$\varepsilon_F = \frac{(1 - B)V\cot\theta_V}{1.2E_S A_{SF}} = \frac{(1 - 0)\,135.5\cot 53.85^\circ}{1.2(29{,}000)(0.44)} = 0.006456$$

$$\varepsilon_{HF} = \sqrt{\varepsilon_H^2 + \varepsilon_F^2} = \sqrt{(0.008849)^2 + (0.006456)^2} = 0.010954$$

$$L_{HF} = 9500\varepsilon_{HF} - 3 = 9500(0.010954) - 3 = 101.06 \text{ in.}$$

$$w = \frac{2.6L_{HF}\varepsilon_{HF}}{(1 + 0.7L_E)^2} = \frac{2.6(101.06)(0.010954)}{(1 + 0.7(29.9))^2} = 0.006 \text{ in. O.K.}$$

The assumed $V_{0.006}$=135.5 kips is correct. If w $\neq$ 0.006 in., then assume another value of $V_{0.006}$ until w = 0.006 in. is reached. The Excel calculation is automatic.

(3) Calculated Output Results

The calculated output of $V_{0.006}$ is shown in a box at the top right corner of the Excel page, together with the design service load V. The ratio of $V_{0.006}$ / V is automatically calculated. If the ratio is greater than or equal to a unity, a "O.K.!" sign will appear. If the ratio is less than unity, a "N.G.!" sign will appear .

The calculated result shows that the existing inverted T beam could not satisfy the serviceability requirement. The allowable service load $V_{0.006}$ based on 0.006 inch crack width is only about 60% of design service load. This explains why large crack can usually be seen in the inverted T-beams for highway bridges. The calculation example for skewed exterior portion of inverted T beam is shown in Fig. 6.7. The crack width at the interior portion of inverted T-beams can be checked directly by Eq. (5.13.2.5.7-1). A calculation example to find $V_{0.0013}$ using spreadsheet trial and error method is shown in Fig. 6.8.

The advantage of using the Excel program is that other variables can be changed to redesign the T-beam, such as increasing the distance from the load V to the end face (L_E), adding diagonal bars, increasing hanger and flexural bars, as well as reducing hanger bar spacing. Examples of such redesign are given in the Appendice.

Acknowledgment

This research is supported by Grant 0-1854 from the Texas Department of Transportation. The project supervisory committee consists of J. C. Liu (Project Coordinator), John P. Vogel (Project Director), Kenneth Ozuna (Project Advisor), Timothy Bradberry (Project Advisor) and Tom Rummel (Project Advisor).

References

AASHTO, (2000). Standard Specifications for Highway Bridges, 16th Ed., American Association of State Highway Transportation Officials Washington D.C.

ACI-318, (1995). Building Code Requirements for Structural Concrete (318-95) and Commentary (318R-95), American Concrete Institute, Farmington Hill, MI.

ACI Committee 224, (2001). Control of Cracking in Concrete Structures. ACI 224R-01

Gibson, J. E. (1992). "Model Analysis and Similitude Requirements," *Small Scale Modelling of Concrete Structures,* Ed. Noor and Boswell, Elsevier Applied Science, London and New York, pp. 13-40.

Mirza S. A. and Furlong R. W. (1983), "Serviceability Behavior and Failure Mechanisms of Concrete Inverted T Beams Bridge Bentcaps ," Journal of American Concrete Institute, July-August 1983/No.4, Proceedings, pp. 294-304

Mirza S. A. and Furlong R. W. (1983), "Strength Criteria for Concrete Inverted T-Girders," Journal of Structural Engineering, ASCE, Vol. 109, No. 8, Aug, 1983, pp. 1836-1853

Mirza S. A. and Furlong R. W. (1985), "Design of Reinforced and Prestressed Concrete Inverted T Beams for Bridge Structures," PCI Journal, Vol. 30, No. 4, July-August, 1985, pp. 112-136

Mirza S. A. and Furlong R. W. (1986), "Design of Reinforced and Prestressed Concrete Inverted T Beams for Bridge Structures," PCI Journal, Vol. 31, No. 3, May-june 1986, pp. 157-163

Muller, R. K. (1992). " Introduction to Modelling of Concrete Structures," *Small Scale Modelling of Concrete Structures,* Elsevier Applied Science, London and New York

Schlaich, J., Schafer, K. and Jennewein, M., (1987). “Toward a Consistent Design of Structural Concrete”, PCI Journal, May-June, pp. 74-150

TxDOT Research Report 0-1854-3, Zhu, R. H., Wanichakorn, W. and Hsu, T. T. C. (2001). “Crack Width Prediction for Interior Portion of Inverted ‘T’ Bent Caps,” Department of Civil and Environmental Engineering, University of Houston, Houston, Texas

TxDOT Research Report 0-1854-4, Zhu, R. H. and Thomas T. C. Hsu (2003) “Crack Width Prediction for Exterior Portion of Inverted ‘T’ Bent Caps” Department of Civil and Environmental Engineering, University of Houston, Houston, Texas

Zhu, R. H., Wanichakorn, W., Hsu, T. T. C. and Vogel, J. (2003) “Crack Width Prediction Using Compatibility-Aided Strut-and-Tie Model,” ACI Structural Journal V. 100, No.4, July-Aug., pp. 413-424

TABLES

Table 2.1 Steel Arrangement and Experimental Loads in Test Specimens

Specimen	f'_c (psi)	Number of Bars				Ultimate Loads (kips)	Service Load (kips)
		Hanger	Flexural	Diagonal	Shear		
BPC1	5,730	6	5	0	3	N/A	198-226
T2	6,054	3	3	0	2	253	94-106
T3	4,865	5	3	0	2	242	111-143
T4	6,011	3	5	0	0	257	111-135
T5	5,649	3	3	3	0	414	128-183
T6	6,283	5	3	0	0	210	104-124
T7	6,826	3	3	5	0	538	167-233

Note: Ultimate loads or service loads are the sum of load V on both sides

Table 2.3 Cracking Width by Prediction and Test at the Mid-point of Service Load Range

Specimen	Steel bar				Service Load (kips)	Test (in.)		Prediction (in.)
	H	F	D	S		E or W Ends	Average	
T2-E	3	3	0	2	100	0.0107	0.0120	0.0120
T2-W	3	3	0	2	100	0.0132		
T3-E	5	3	0	2	127	0.0107	0.0127	0.0126
T3-W	5	3	0	2	127	0.0146		
T4-E	3	5	0	0	123	0.0099	0.0135	0.0148
T4-W	3	5	0	0	123	0.0170		
T5-E	3	3	3	0	156	0.0100	0.0099	0.0105
T5-W	3	3	3	0	156	0.0097		
T6-E	5	3	0	0	114	0.0093	0.0096	0.0093
T6-W	5	3	0	0	114	0.0099		
T7-E	3	3	5	0	200	0.0103	0.0113	0.0102
T7-W	3	3	5	0	200	0.0123		

Note: Service loads are the sum of load V on both sides

Table 3.1 Loads and Crack Widths in Test Specimens

Specimen	f'_c (psi)	Crack Width at Nominal Shear Resistance V_n for Service Limit State (in.)		Nominal Shear Resistance V_n for Service Limit State (kips) Eqs.(3.1) & (3.2)	Ultimate Test Load V (kips)
		C2	C3		
E-0-6	5024	0.0031	0.0034	27.9	75.8
E-0-10	6182	0.0039	0.0053	46.5	98.1
E-0-12	5876	0.0024	0.0039	55.8	130.7
E-0-14	5801	0.0049	0.0063	50.6	117.8
E-0-18	5748	0.0002	0.0007	50.6	135.1
E-0-20	6056	0	0.0005	56.4	151.7*
E-1-10	5065	0.002	0.003	46.5	97.6
E-2-6	5204	0.0013	0.0018	27.9	77.3
E-2-10	6764	0.0025	0.0028	46.5	113.7
E-5-12	4611	0.0011	0.0022	55.8	115.6

* Premature failure at the other end of specimen.

Table 3.3 Loads $V_{0.004}$ and $V_{0.007}$ Corresponding to Crack Widths of 0.004 in. and 0.007 in.

Specimen	Test (kips)			Prediction (kips)			$V_{0.004}$	$V_{0.007}$
	$V_{0.004}$	$V_{0.007}$	ΔV	$V_{0.004}$	$V_{0.007}$	ΔV	$\frac{V_{test}-V_{pred.}}{V_{test}}\times 100$	$\frac{V_{test}-V_{pred.}}{V_{test}}\times 100$
E-0-6	29.0	32.0	3.0	29.9	30.8	0.6	-3.1	3.8
E-0-10	46.9	48.2	1.3	47.4	49.4	2.0	-1.1	-2.5
E-0-12	61.0	61.7	0.7	54.2	57.1	2.9	11.1	7.5
E-0-14	49.4	51.7	2.3	62.3	66.1	3.9	-26.1	-27.9
E-0-18	82.2	87.9	5.7	84.8	91.3	6.5	-3.2	-3.9
E-0-20	98.4	101.3	2.9	94.6	102.6	8.0	3.9	-1.3
E-1-10	49.9	51.0	1.1	48.6	51.0	2.4	2.6	0.0
E-2-6	38.1	40.3	2.2	36.1	38.8	2.7	5.2	3.7
E-2-10	53.9	60.5	6.6	55.4	59.4	4.0	-2.8	1.8
E-5-12	65.0	69.5	4.5	66.8	74	7.2	-2.8	-6.5

Table 4.2 Whole Specimens (inch)

Specimen	North Part					South Part				
	Edge Distance L_E of Load V	Number of Diagonal Bar at End Face	Hanger Spacing at End Face	Hanger Spacing Under Actuator B	Loading Pad Under Actuator B	Edge Distance L_E of Load V	Number of Diagonal Bars at End Face	Hanger Spacing at End Face	Hanger Spacing under Actuator C	Loading Pad Under Actuator C
W1	14	2	4	4	10 × 6	14	4	4	4	6 × 6
W2	14	2	5.5	5.5	10 × 6	14	2	2.5	5.5	6 × 6

Table 4.3.3(a) Calculation of Distribution Width for W1-B

Load V (kips)	Hanger Bar Force (kips)							$\sum_{i=1}^{7} F_i$ (kips)	$L_D = \frac{2\sum_{i=1}^{7} F_i}{\frac{F_7'}{S}}$ (inch)	$x = \frac{L_D - W}{d_e}$
	F_7'	F_6	F_5	F_4	F_3	F_2	F_1			
80	6.6	5.1	3.1	1.0	0.6	0.2	0.0	16.6	20.2	0.92
90	10.4	8.2	4.8	1.4	0.9	0.3	0.2	26.2	20.1	0.92
100	14.2	12.6	7.6	2.7	1.5	0.3	0.2	39.1	22.0	1.09
110	18.0	18.0	12.5	4.5	2.4	0.3	0.2	55.8	24.8	1.35
120	18.0	18.0	18.0	6.2	3.1	-0.1	-0.2	63.2	28.1	1.65
123	18.0	18.0	18.0	8.7	4.2	-0.2	-0.3	66.8	29.7	1.79

Note: S = 4 inch, W = 10 inch, d_e = 11 inch.

The hanger bar forces (F) are calculated from the measured strains using E_s = 29,000 ksi and A_s = 0.31 in.^{2}, up to an assumed yield force of 18.0 kips.

F_7' = average of F_7 and F_8.

Strain of B5 = average strain of B6 and B4, Strain of B3 = average strain of B4 and B2.

Table 4.3.3(b) Calculation of Distribution Width for W1-C

Load V (kips)	Hanger Bar Force (kips)							$\sum_{i=1}^{7} F_i$ (kips)	$L_D = \frac{2\sum_{i=2}^{7} F_i}{\frac{F_7'}{S}}$ (inch)	$x = \frac{L_D - W}{d_e}$
	F_7'	F_6	F_5	F_4	F_3	F_2	F_1			
70	2.6	1.4	1.0	0.6	0.4	0.1		6.1	18.9	1.17
80	10.7	6.8	4.1	1.4	0.8	0.1		23.8	17.9	1.08
90	17.8	12.4	7.4	2.4	1.4	0.5		41.9	18.8	1.16
100	18.0	15.4	9.6	3.8	2.1	0.3		49.2	21.9	1.45
110	18.0	18.0	18.0	9.2	4.7	0.3		68.2	30.3	2.21

Note: S = 4 inch, W = 6 inch, d_e = 11 inch,

F_7' = average of F_7 and F_8,

Strain of B5 = average strain of B6 and B4, Strain of B3 = average strain of B4 and B2

Table 4.3.3(c) Calculation of Distribution Width for W2-B

Load V (kips)	Hanger Bar Force (kips)					$\sum_{i=1}^{5} F_i$ (kips)	$L_D = \frac{2\sum_{i=1}^{5} F_i}{\frac{F'_5}{S}}$ (inch)	$x = \frac{L_D - W}{d_e}$
	F'_5	F_4	F_3	F_2	F_1			
70	1.9	0.8	0.3	0.0	0.0	3.0	17.2	0.66
80	8.5	4.7	1.9	0.0	0.3	15.4	19.9	0.90
90	15.2	10.4	3.7	0.0	0.4	29.6	21.4	1.04
100	18.0	18.0	6.0	0.0	0.5	42.4	25.9	1.45
103	18.0	18.0	6.2	0.0	0.5	42.7	26.1	1.47

Note: S = 5.5 inch, W = 10 inch, d_e = 11 inch

F'_5 = average of F_5 and F_6

Table 4.3.3(d) Calculation of Distribution Width for W2-C

Load V (kips)	Hanger Bar Force (kips)					$\sum_{i=1}^{5} F_i$ (kips)	$L_D = \frac{2\sum_{i=1}^{5} F_i}{\frac{F'_5}{S}}$ (inch)	$x = \frac{L_D - W}{d_e}$
	F'_5	F_4	F_3	F_2	F_1			
80	5.6	6.3	2.6	0.6	0.5	15.6	30.5	2.22
90	10.7	12.1	5.9	0.8	0.6	30.2	30.9	2.27
100	16.1	15.1	7.4	0.0	0.6	39.2	26.7	1.88
113	18.0	18.0	13.4	0.0	0.9	50.2	30.7	2.25

Note: S = 5.5 inch, W = 6 inch, d_e = 11 inch

F'_5 = average of F_5 and F_6

Table 4.4(a) Comparison of Test Specimen and Prototype (inch)

	Spring Cypress Overpass inverted T beam	Test Specimen Inverted T beam	Scale Ratio
Total height of inverted T beam	71	26	2.7
Total width of inverted T beam	83	42	2.0
Ledge height (h)	21	13	1.6
Ledge cantilever Length	16	10.5	1.5
height measured from the centroid of bottom flexural bar to the centriod of top flexural bar	16.25	9	1.8
Distance from load V to center of hanger bar a_f	11.9	7.25	1.6
Hanger bar diameter	0.75	0.625	1.2
Flexural bar diameter	0.75	0.625	1.2
Hanger bar spacing	4.1	4	1.0
Flexural bar spacing	4.1	4	1.0
Concrete clear cover	2	1.69	1.2
Distance from load to edge L_E	29.9	6 to 20	5 to 1.5
Design Service Load for prototype and $V_{0.004}$ for specimens when crack opens up very fast (kips).	221	29 to 98.4	7.6 to 2.2

Table 4.4(b) Dimensions of Physical Quantities

Quantity	Relationship	Absolute System	Engineering System
Length		L	L
Mass M		M	$FL^{-1}T^{-2}$
Velocity	Displacement / time	LT^{-1}	LT^{-1}
Acceleration	Velocity / time	LT^{-2}	LT^{-2}
Force F	Mass × acceleration	MLT^{-2}	F
Stress	Force / area	$ML^{-1}T^{-2}$	FL^{-2}
Strain	= u / L	----	-----
Modulus of Elasticity E	Force / area	$ML^{-1}T^{-2}$	FL^{-2}

Table 4.4(c) Dimensions and Scaling Factors of Physical Quantities

Quantity	Dimensions	Engineering System
Modulus of Elasticity	FL^{-2}	S_E
Stress	FL^{-2}	S_E
Strain	---	1
Length	L	S_ℓ
Displacement	L	S_ℓ
Area	L^2	S_ℓ^2
2^{nd} moment of area	L^4	S_ℓ^4
Concentrated Load	F	$S_E S_\ell^2$
Moment	FL	$S_E S_\ell^3$
Shear	F	$S_E S_\ell^2$

Table 4.4(d) Crack Width of Inverted T Beam in the Bridge at Laura Koppe Road

Girder Span (ft)	124
Girder Spacing (ft)	9.94
Normal distance from load V to web edge a_V (in)	8.52
Distance from Load V to end face L_E (in)	22
Hanger Bar Area A_{SH} (in^2)	0.44
Flexural Bar Area A_{SF} (in^2)	0.6
Skew Angle θ (degree)	1.53
Ledge Height h (in)	21.96
$V_{0.006}$ (kips) Eq. (4.6)	114.3
Service Load V (kips)	273
Predicted Crack Width at Service Load (in) Eq. (4.7)	0.083
Maximum Measured Crack Width at Service Load (in)	0.09

FIGURES

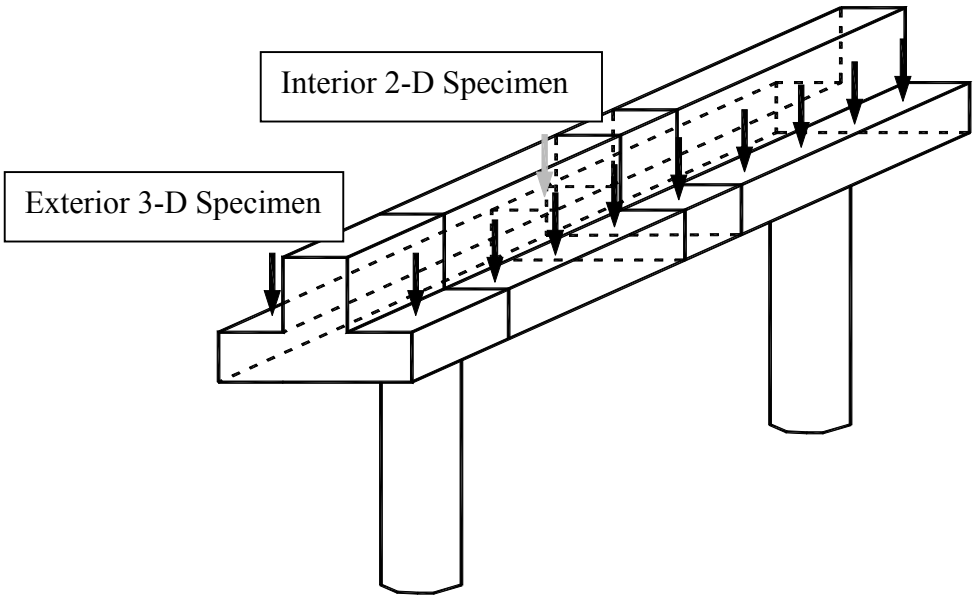

Fig. 1(a) An inverted 'T' bent cap showing an exterior 3-D specimen and an interior 2-D specimen

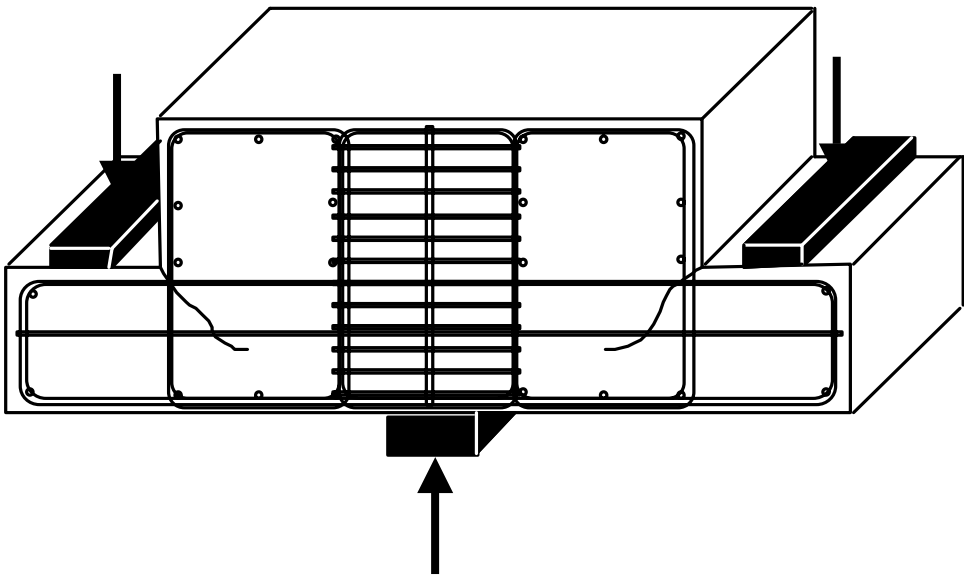

Fig. 1(b) 2-D Test Specimen

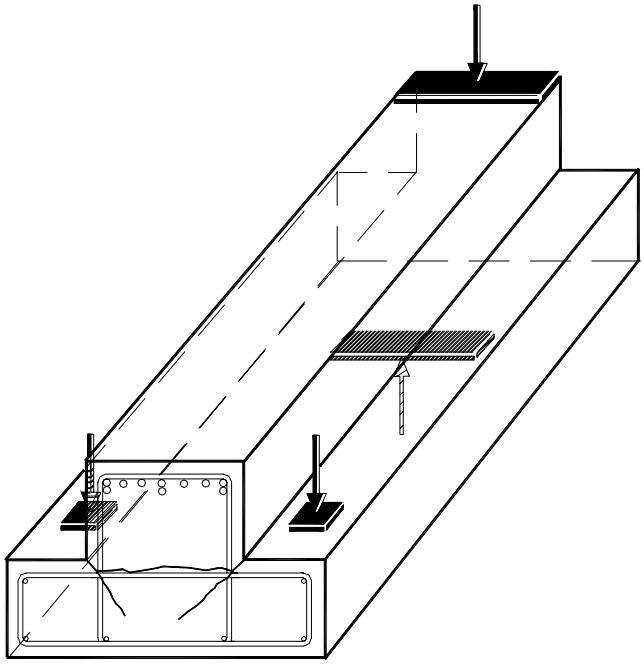

Fig. 1(c) 3-D Test Specimen

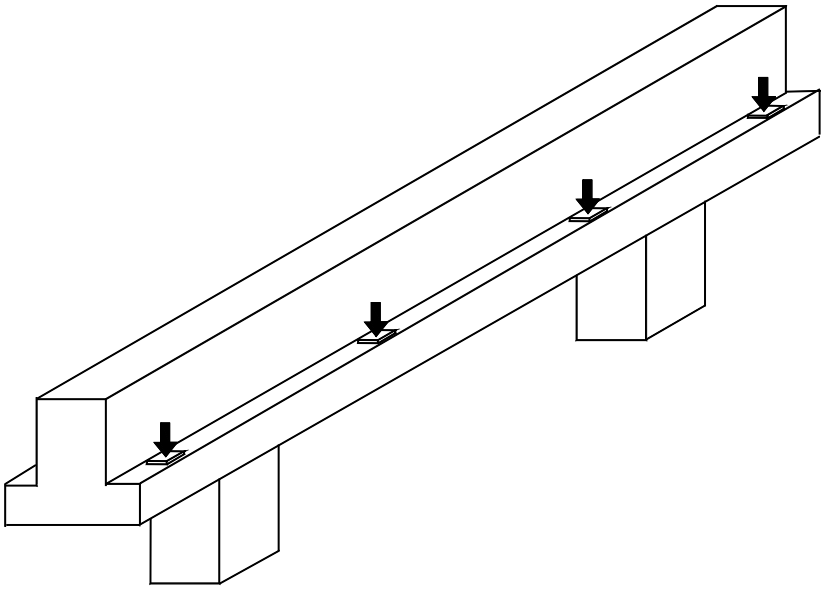

Fig. 1(d) Tests of Whole Inverted T Bent Caps

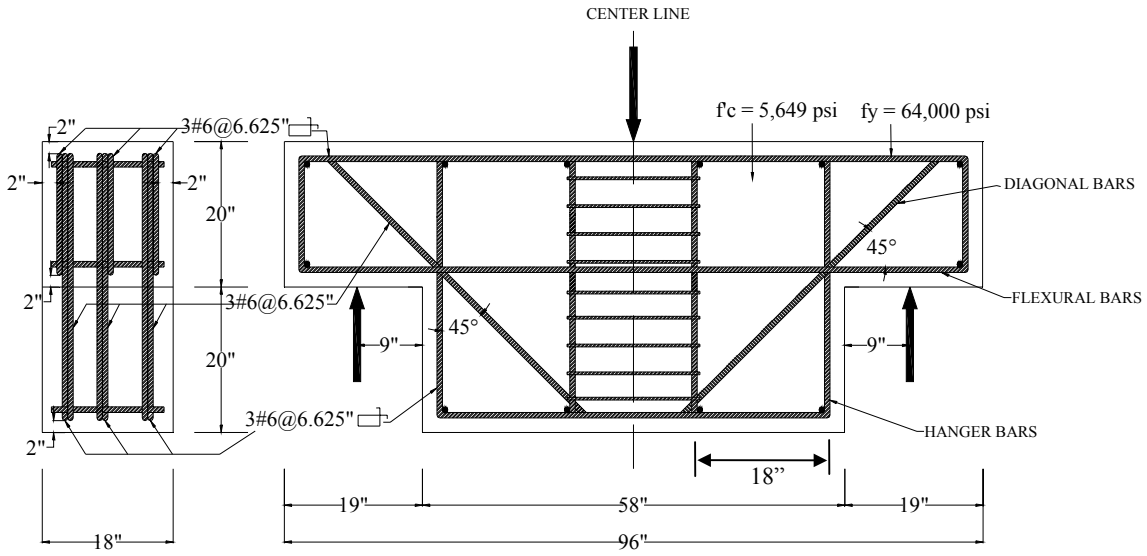

Fig. 2.1(a) Dimensions and steel arrangement of Specimen T5

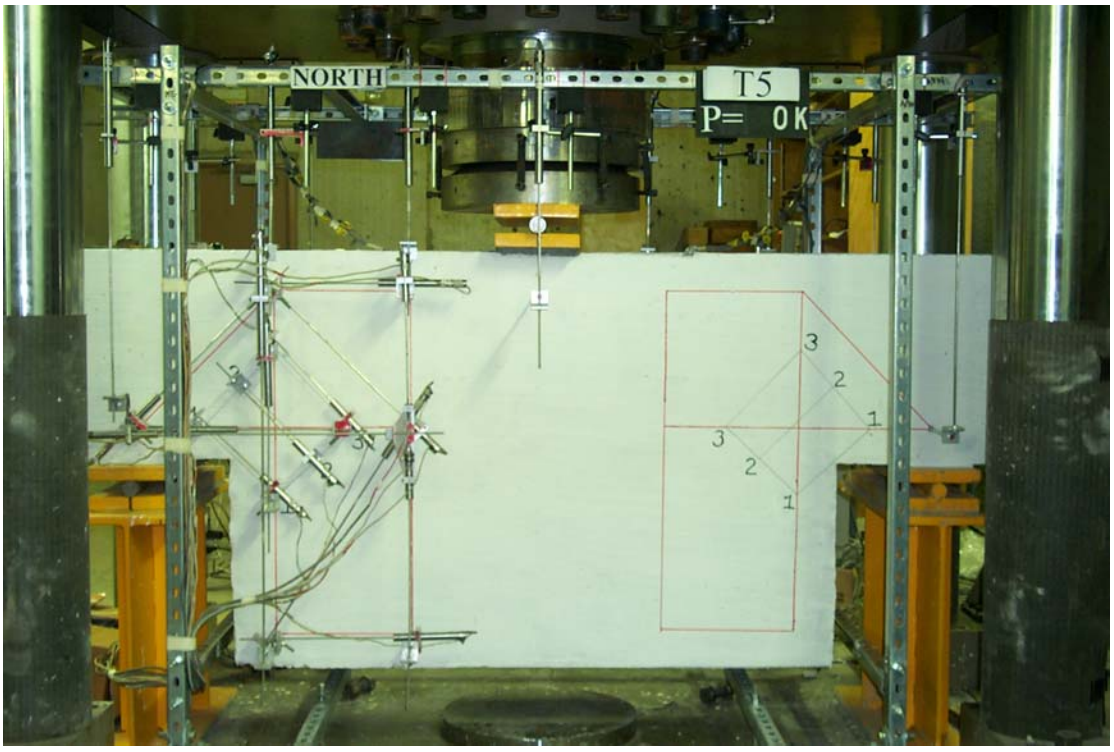

Fig. 2.1(b) Test setting-up of Specimen T5

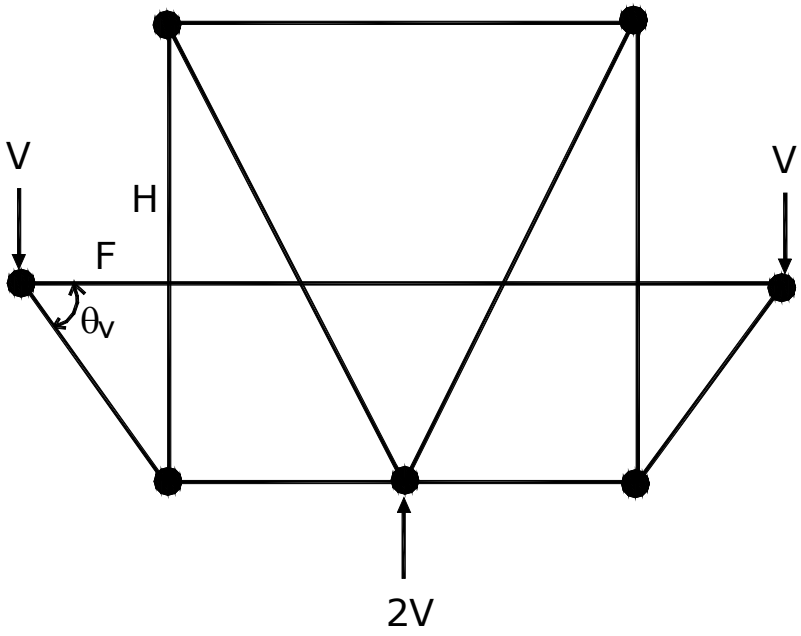

Fig. 2.2(a) CASTM model without diagonal bars

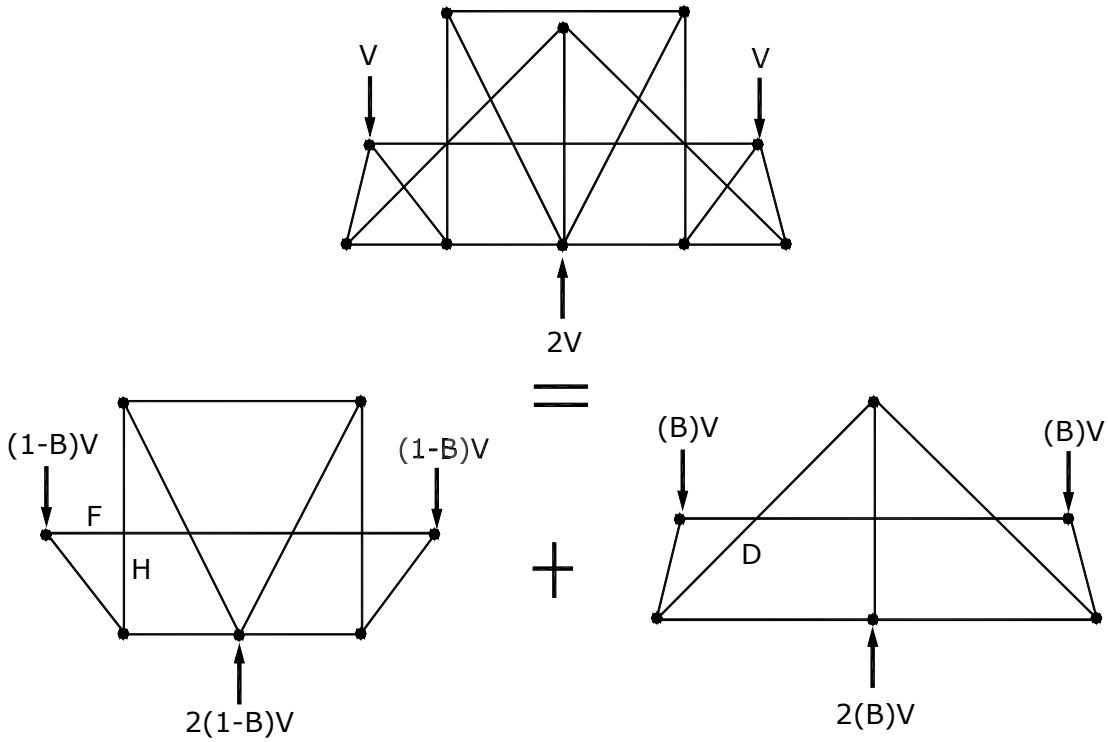

Fig. 2.2(b) CASTM model with diagonal bars

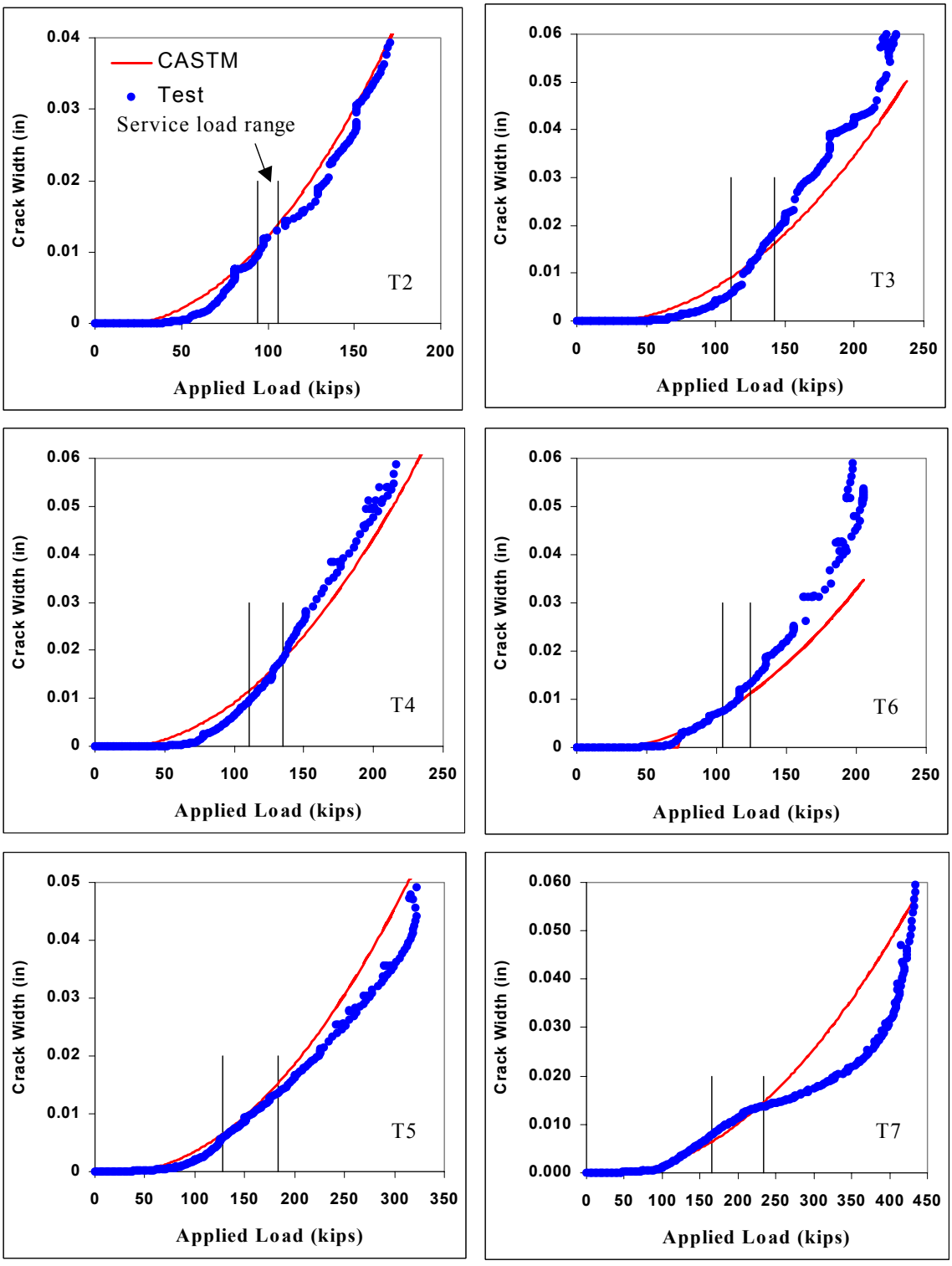

Fig. 2.3(a) Comparison of CASTM with tests

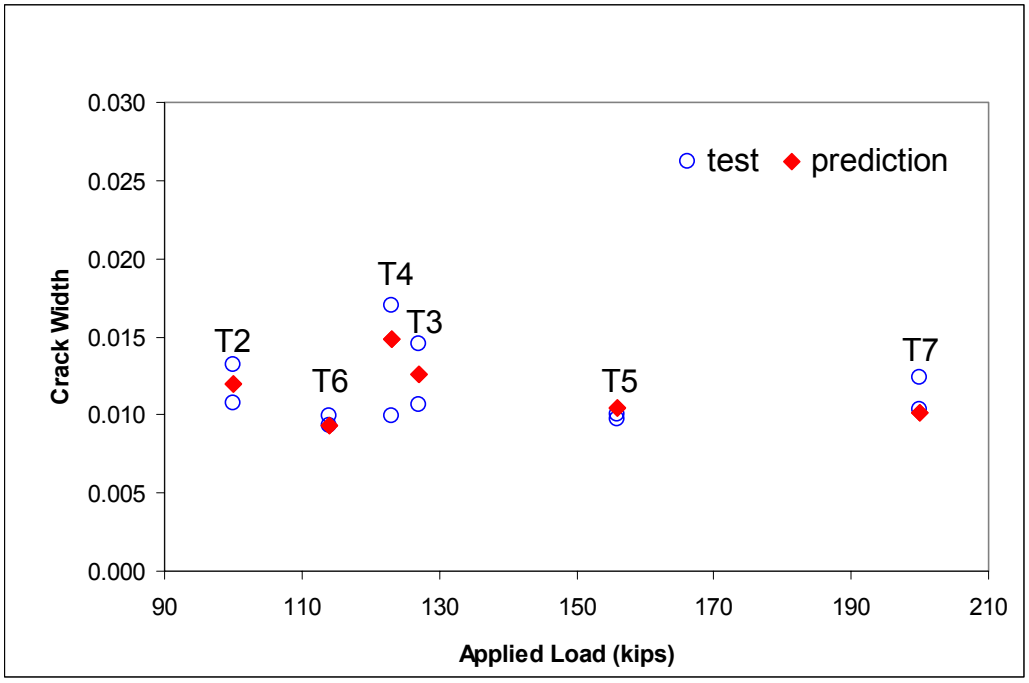

Fig. 2.3(b) Comparison of crack width by CASTM and the tests

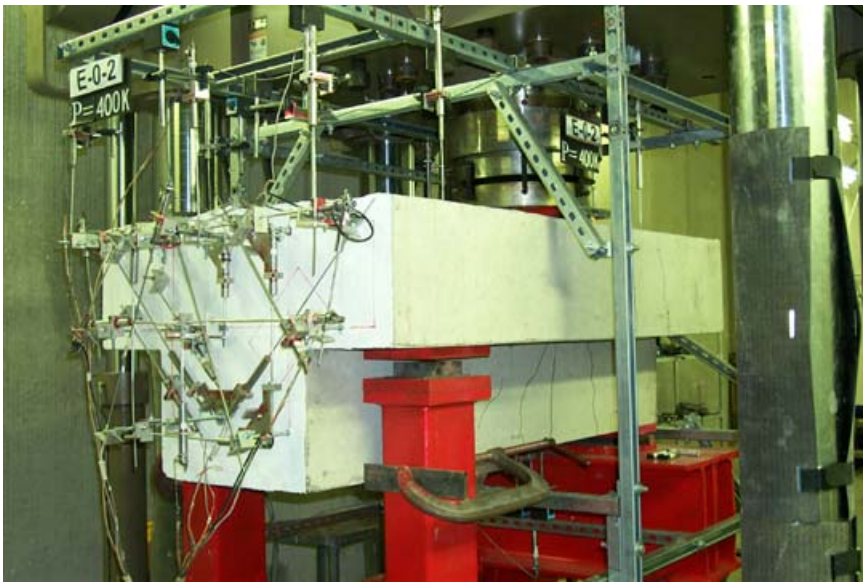

Fig. 3.1(a) General view of test set-up

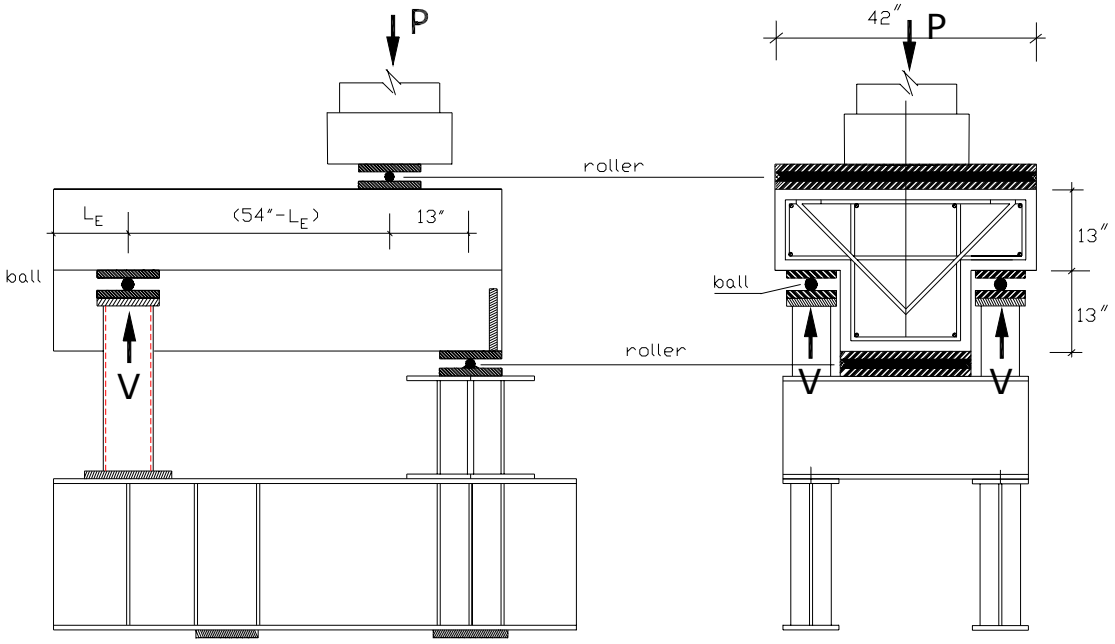

Fig. 3.1(b) Arrangement and dimension of test set-up

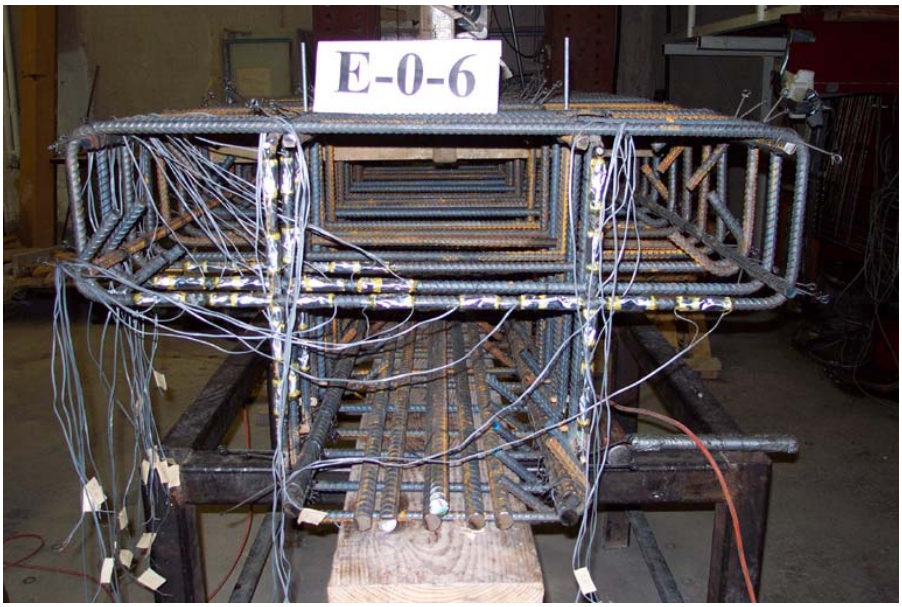

Fig. 3.1(c) Steel cage without diagonal bars (Specimen E-0-6)

Fig. 3.1(d) Steel cage with two diagonal bars (Specimen E-2-6)

Fig. 3.1(e) LVDTs to study the variation of hanger steel strains along the span

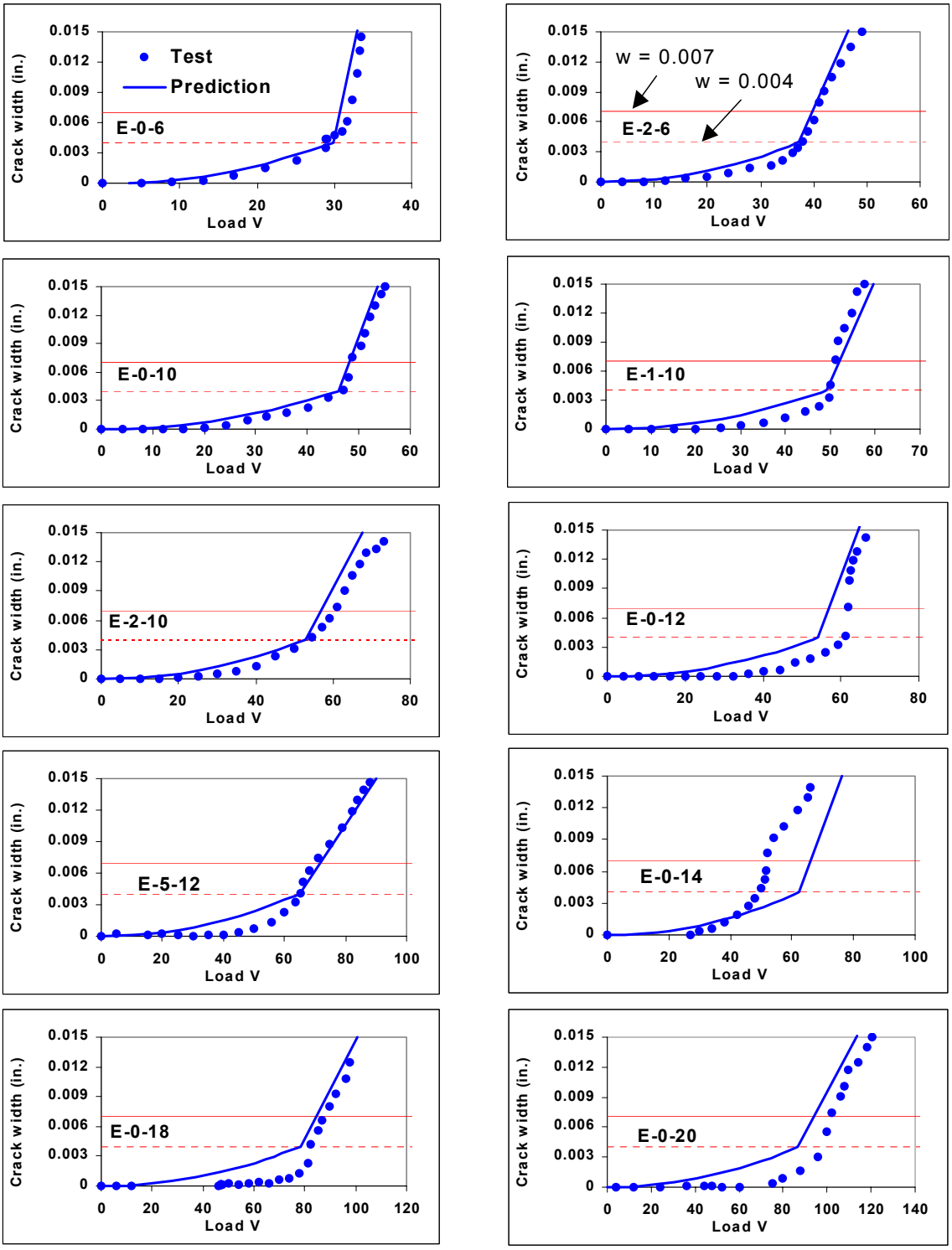

Fig. 3.3 Comparison of tests and predictions

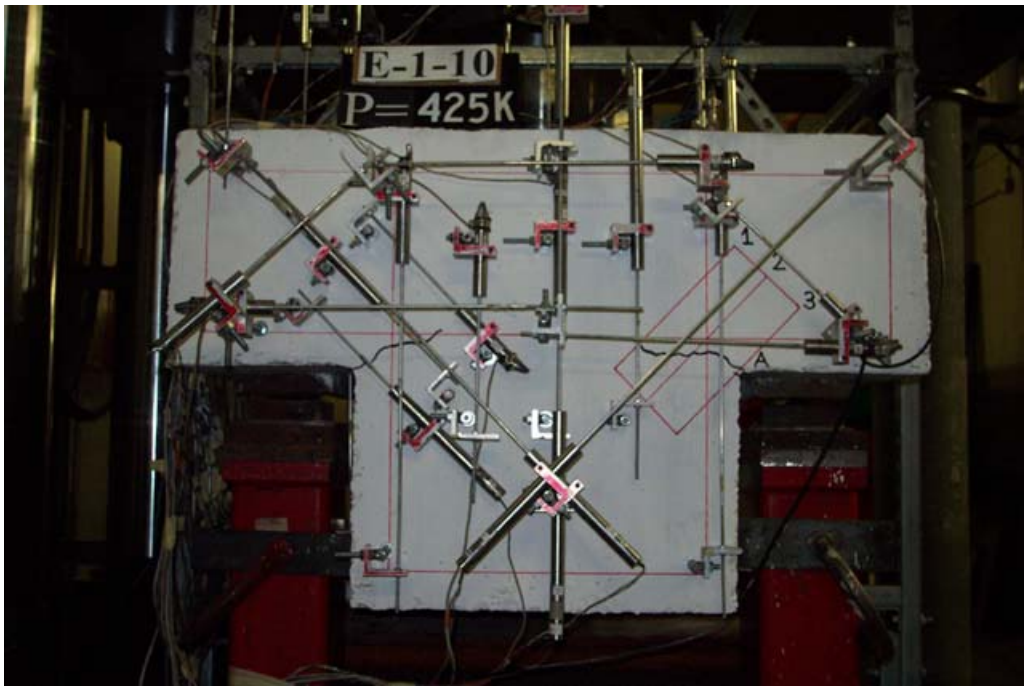

Fig. 3.4(a) Crack pattern when w is less than 0.004 inch

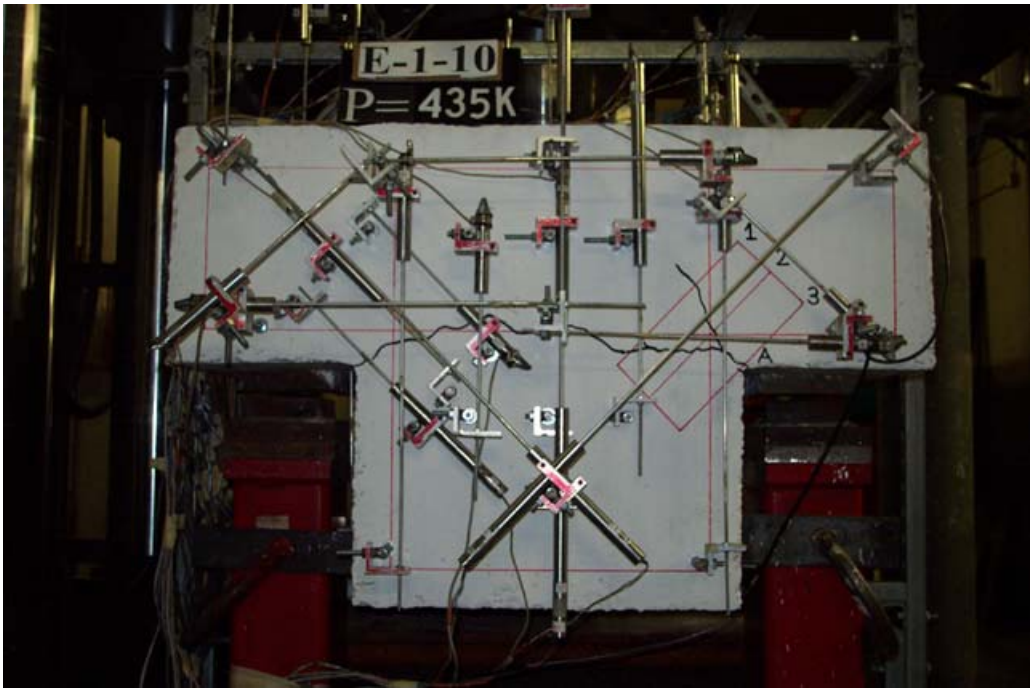

Fig. 3.4(b) Crack pattern when w is larger than 0.004 inch

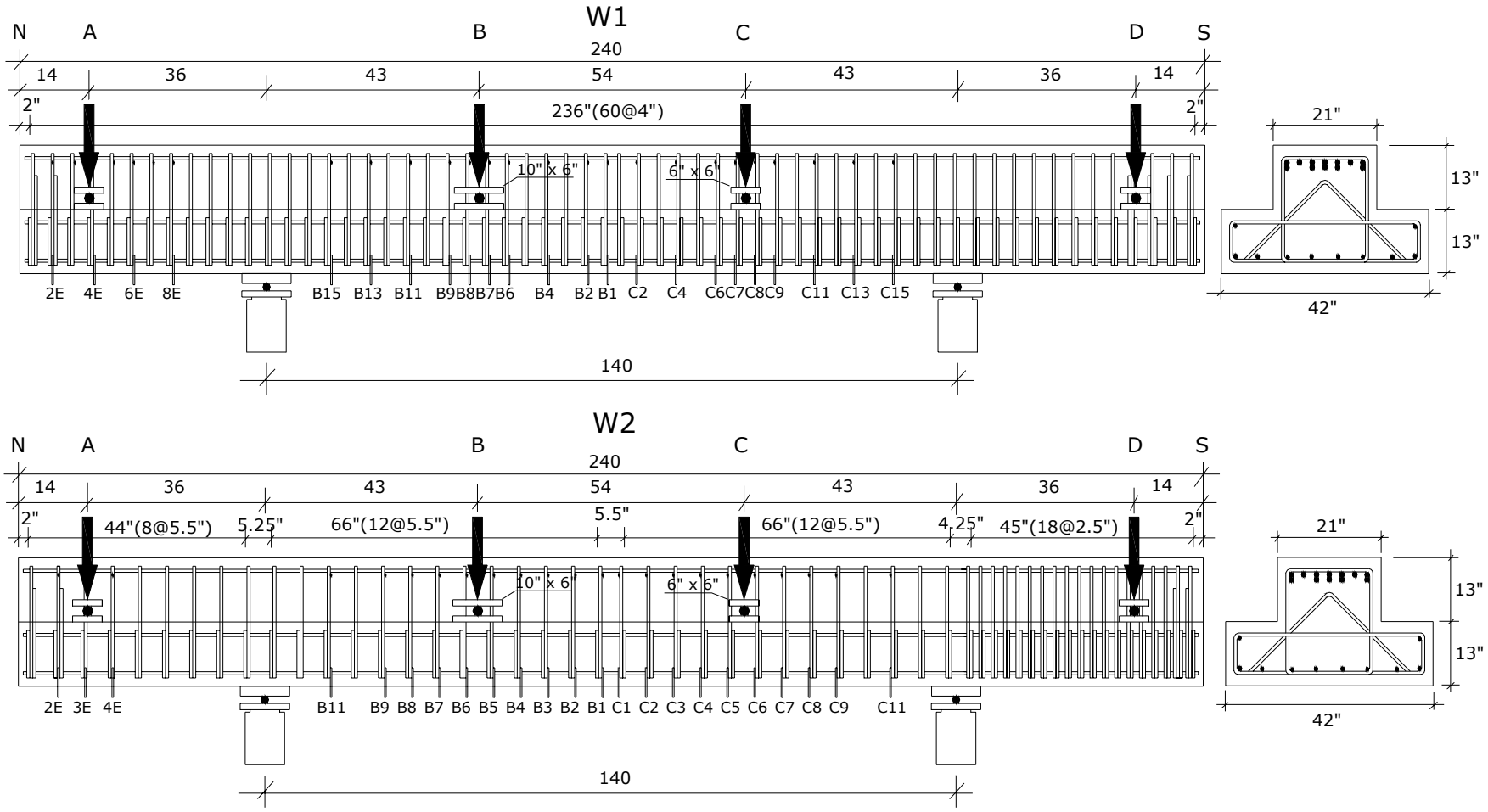

Fig. 4.2.1 Whole specimens

Fig. 4.2.2(a) Test frame setup with specimen

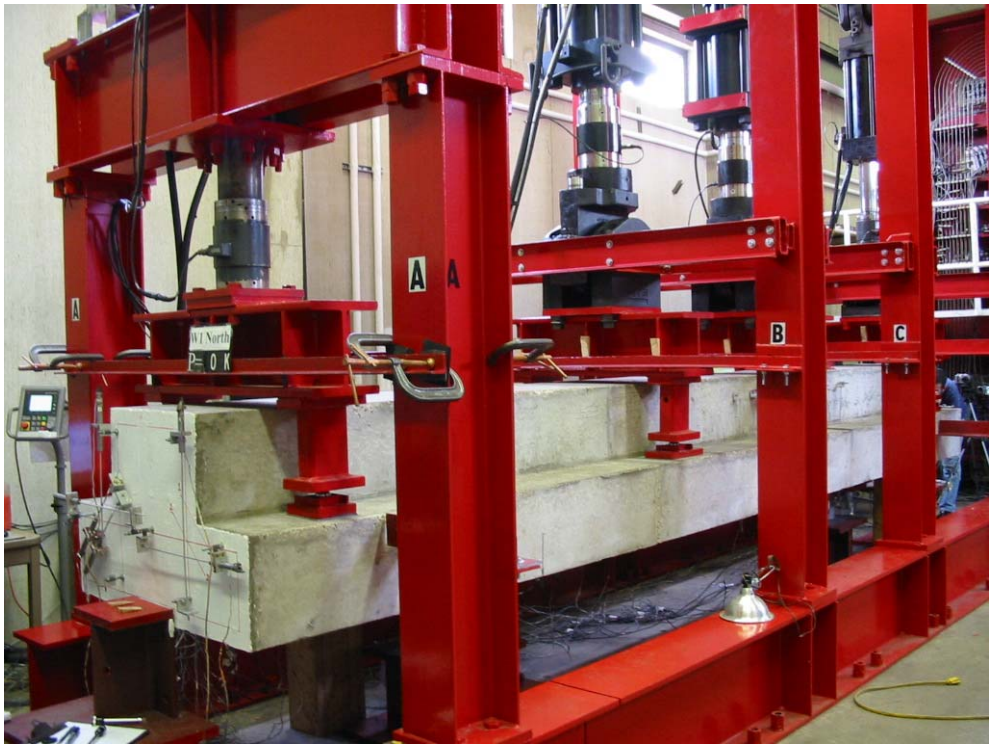

Fig. 4.2.2(b) Actuators A, B, C and D with whole specimen

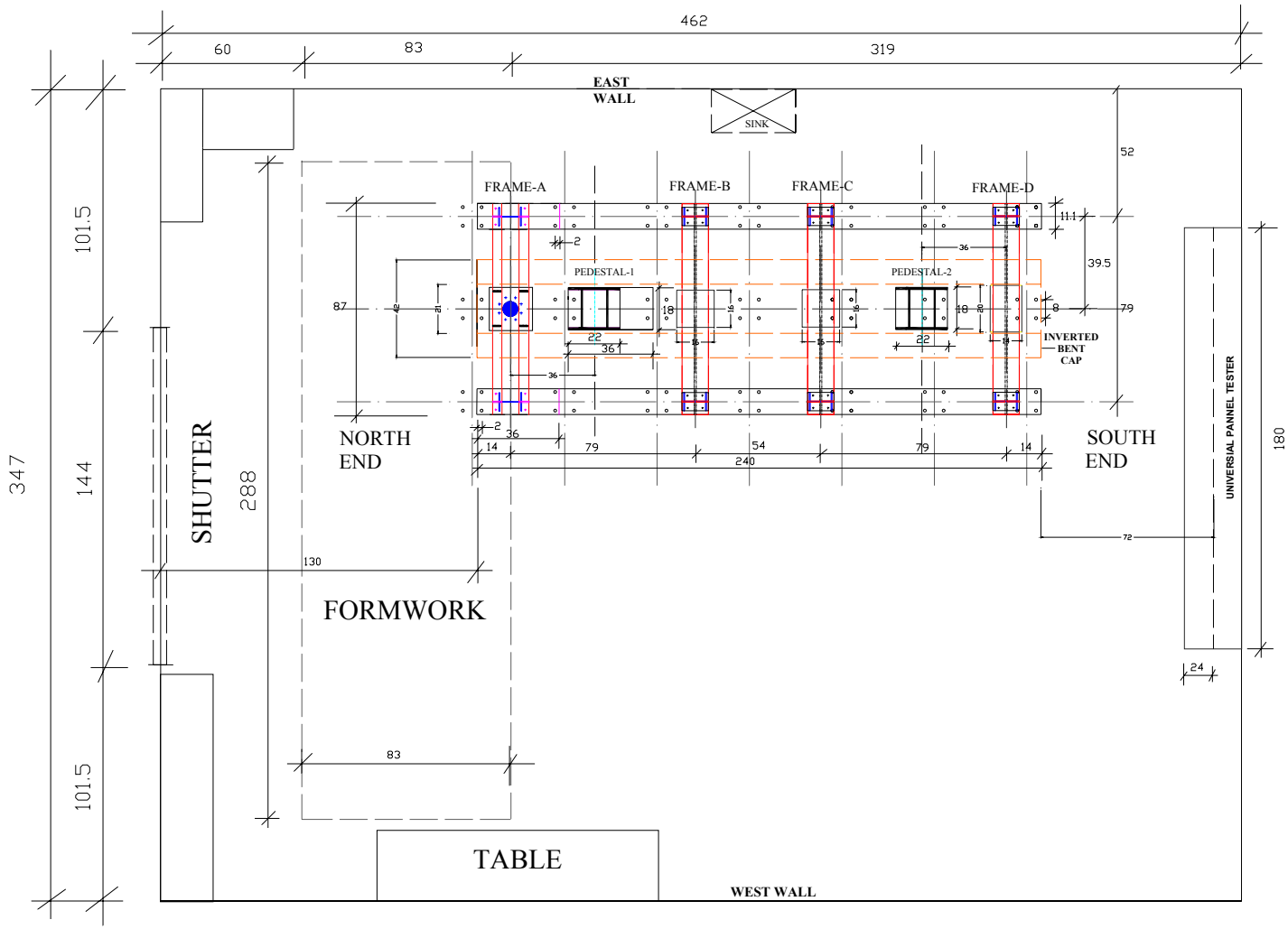

Fig. 4.2.3(a) Horizontal plan of test frame

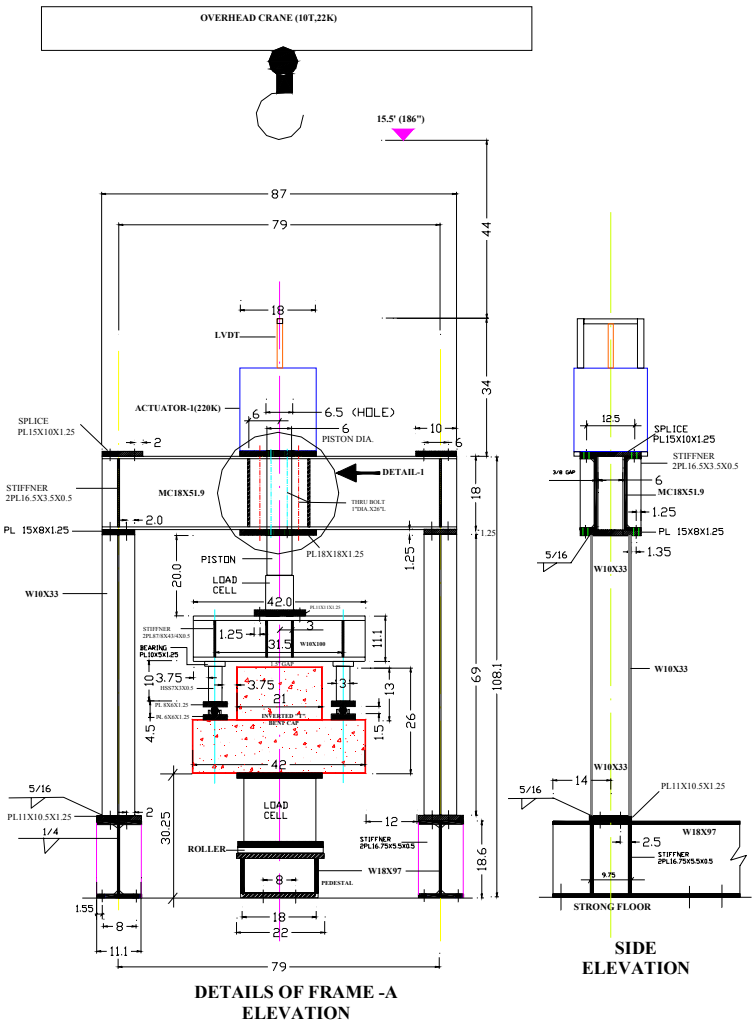

Fig. 4.2.3(b) Vertical Frame A

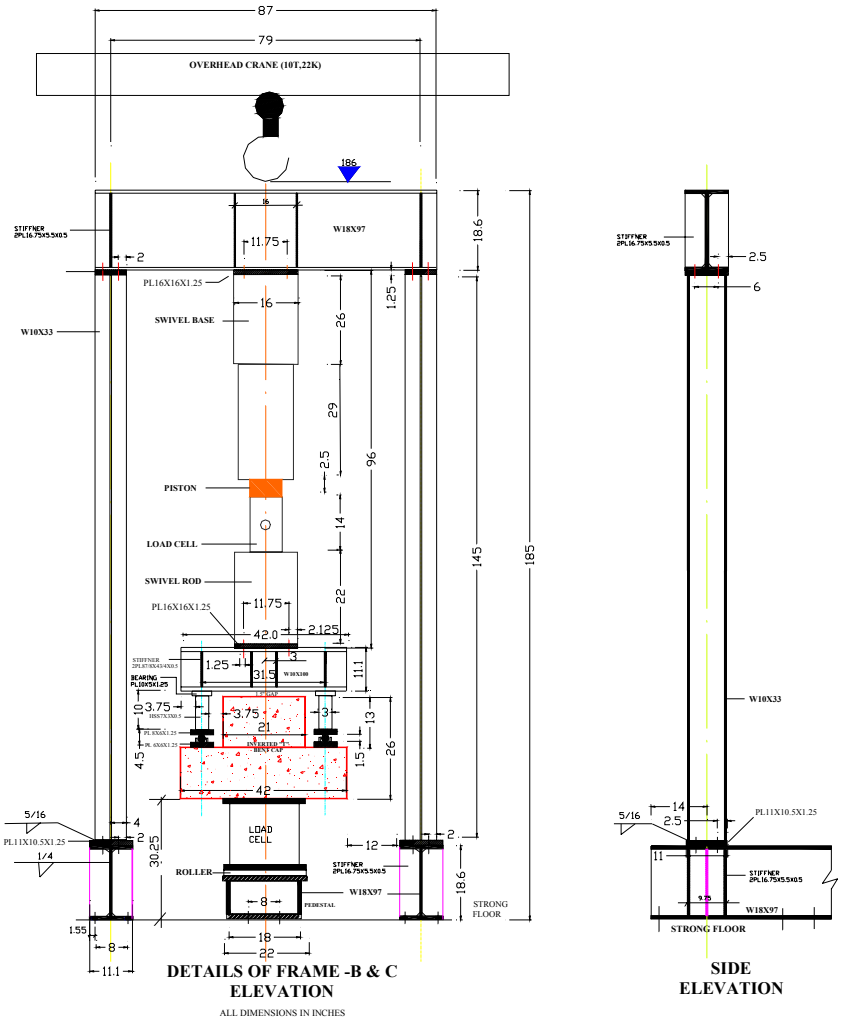

Fig. 4.2.3(c) Vertical Frame B & C

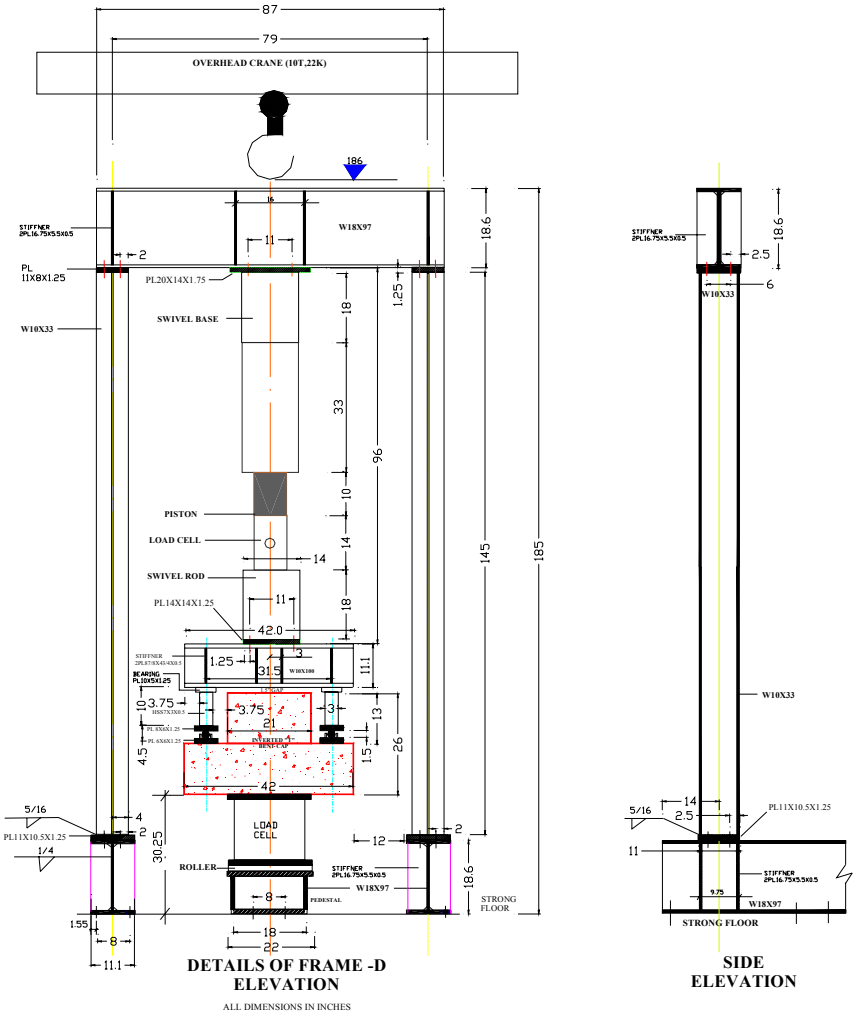

Fig. 4.2.3(d) Vertical Frame D

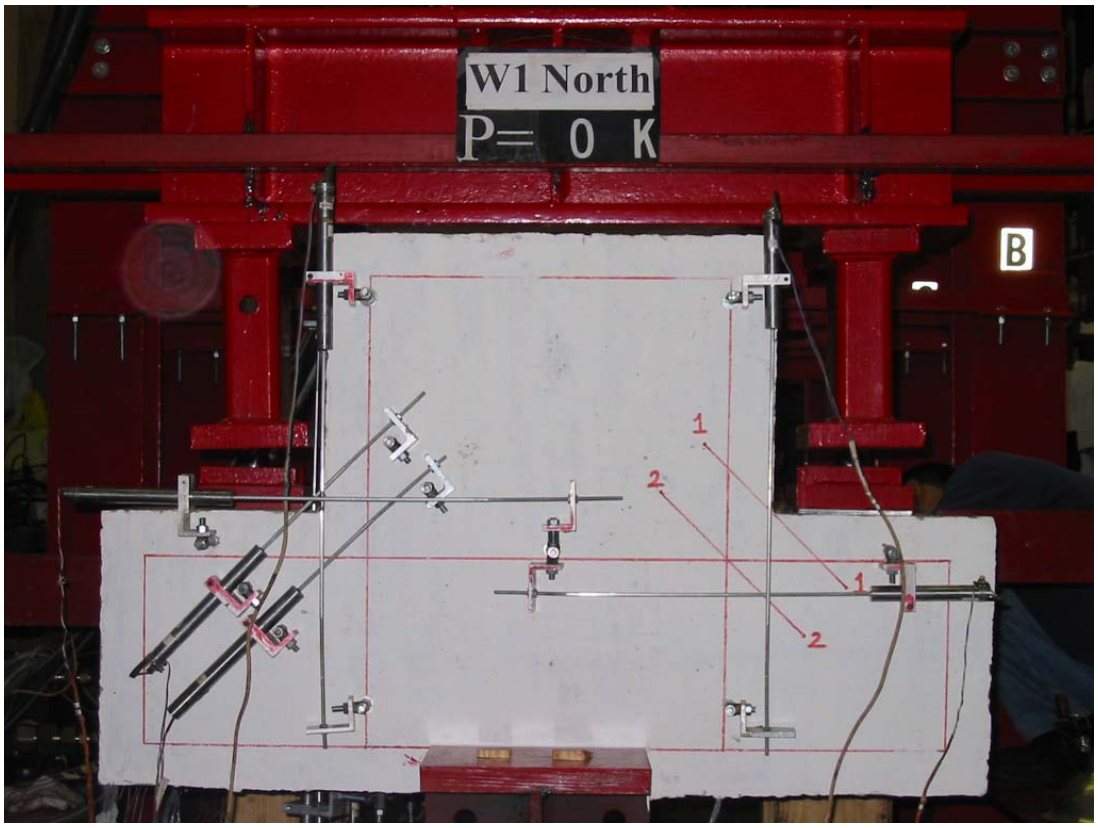

Fig. 4.2.4(a) Arrangement of LVDTs on end face

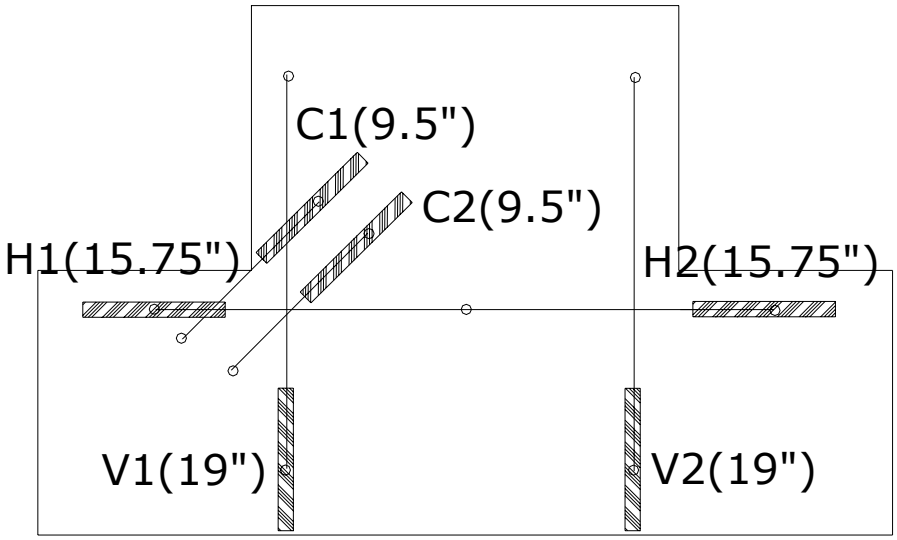

Fig. 4.2.4(b) Labeling of LVDTs on end face

Fig. 4.2.4(c) LVDTs to study effective distribution width L_D along span

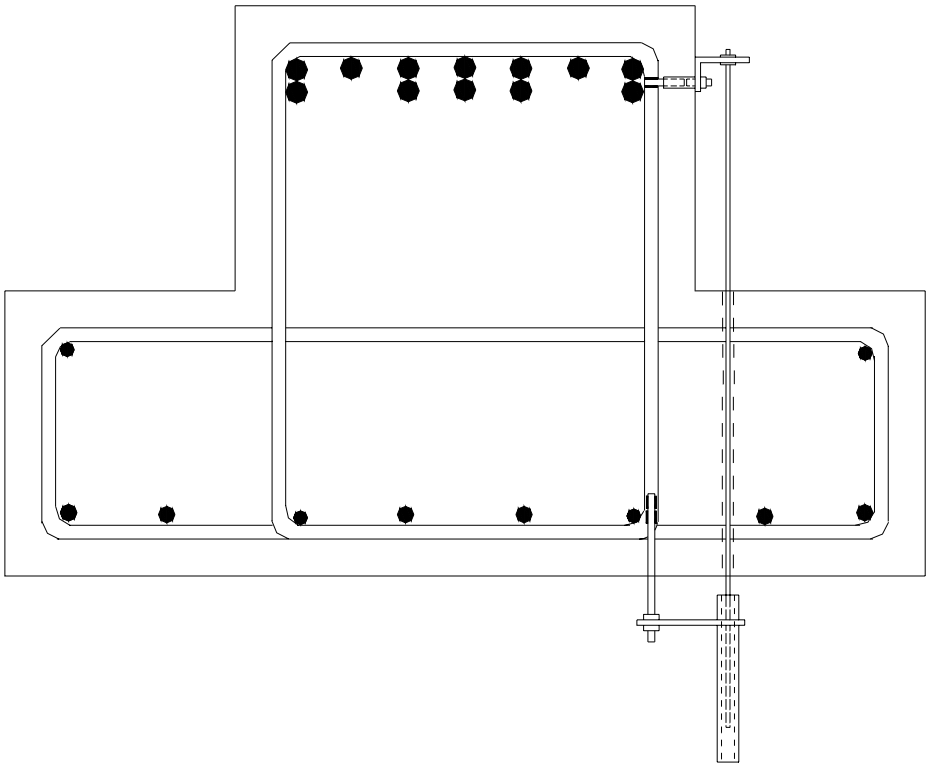

Fig. 4.2.4 (d) Special arrangement of LVDT to measure strain variation of hanger along span

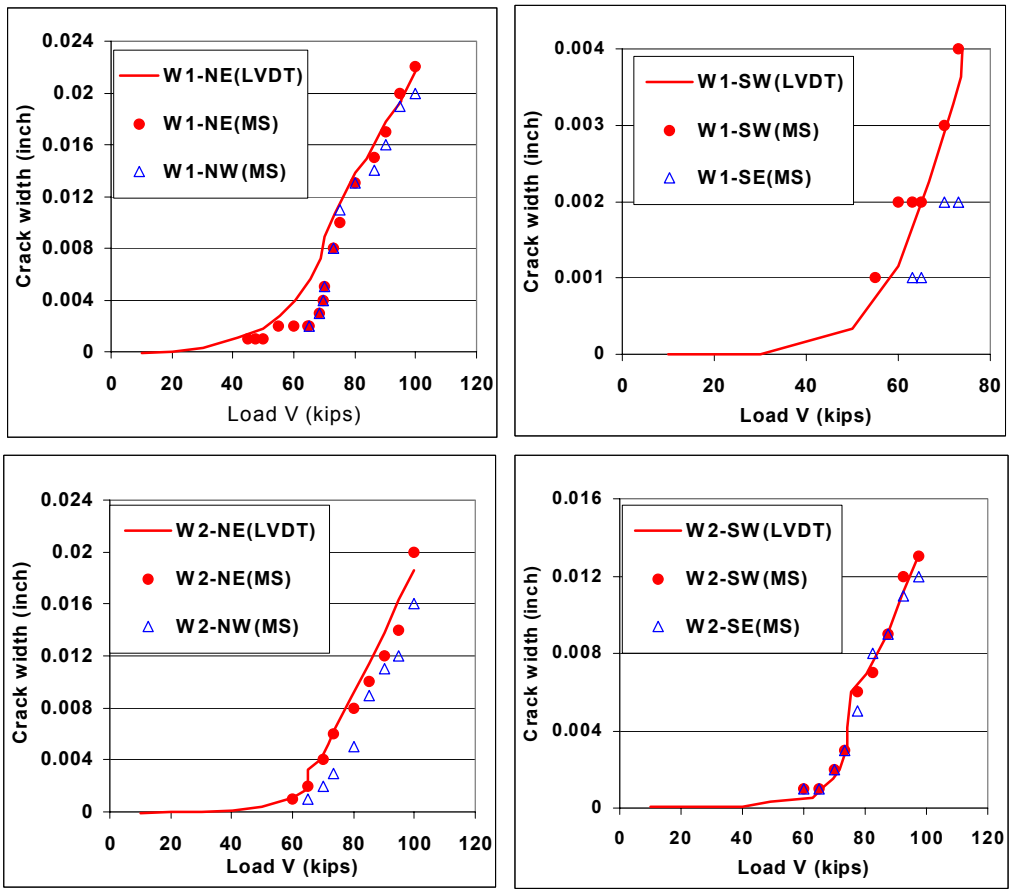

Fig 4.3.1(a) Crack width measured by microscope and LVDT

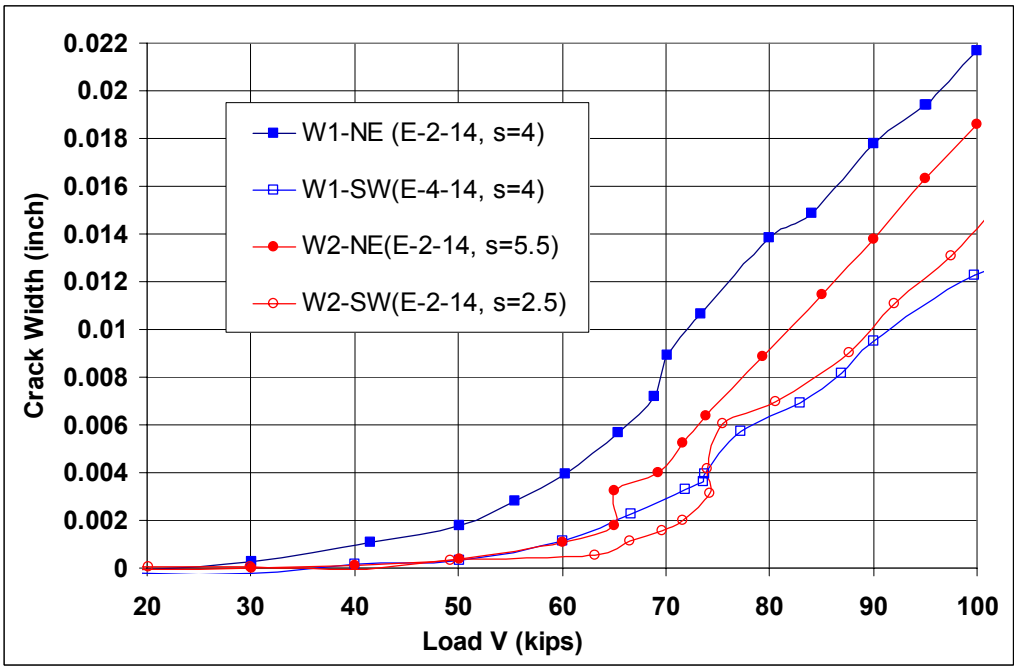

Fig 4.3.1(b) Crack width vs. load

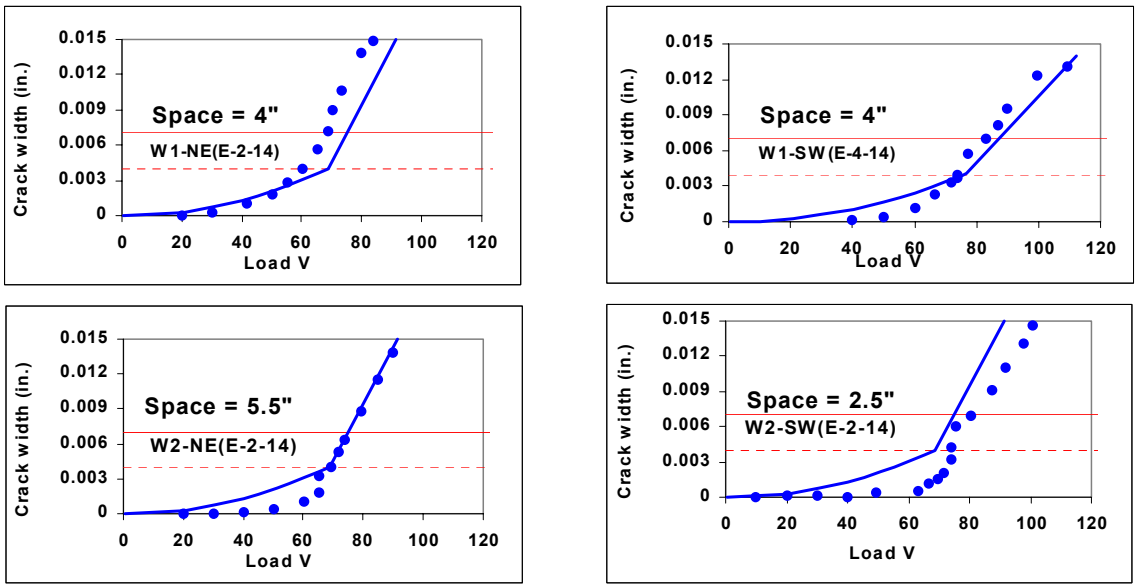

Fig 4.3.1(c) Comparison of prediction with tests

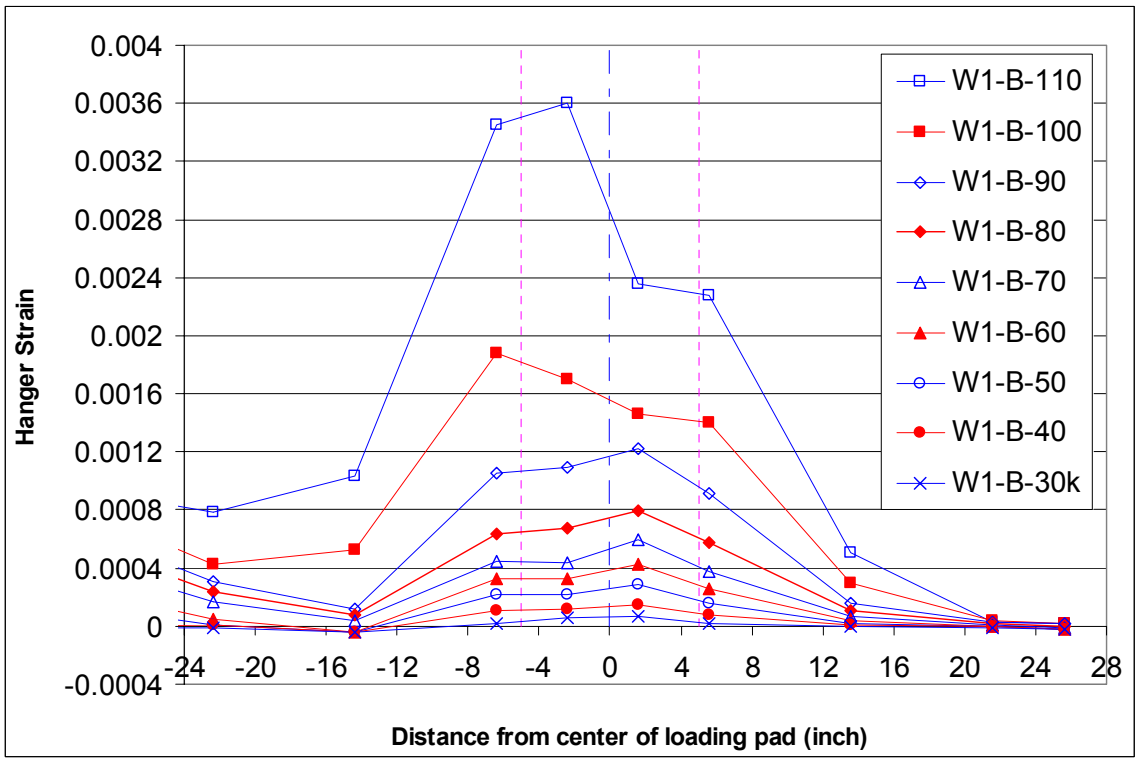

Fig. 4.3.2(a) Hanger strain variation along span (W1-B)

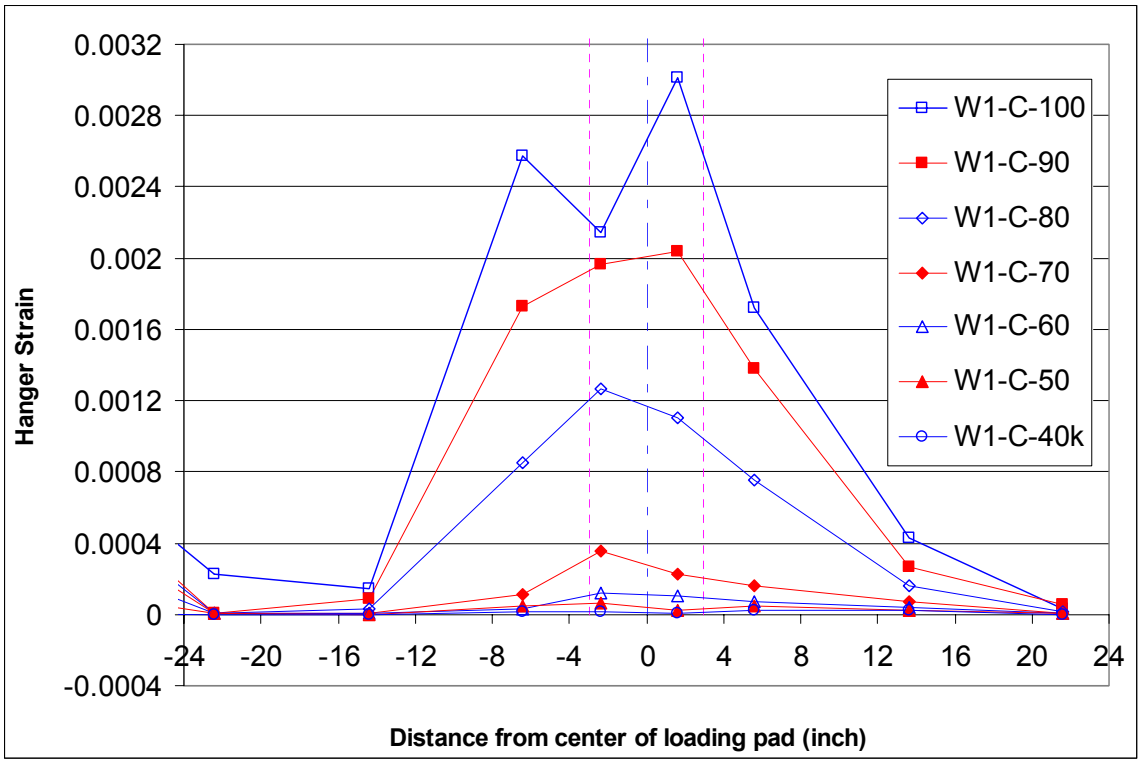

Fig. 4.3.2(b) Hanger strain variation along span (W1-C)

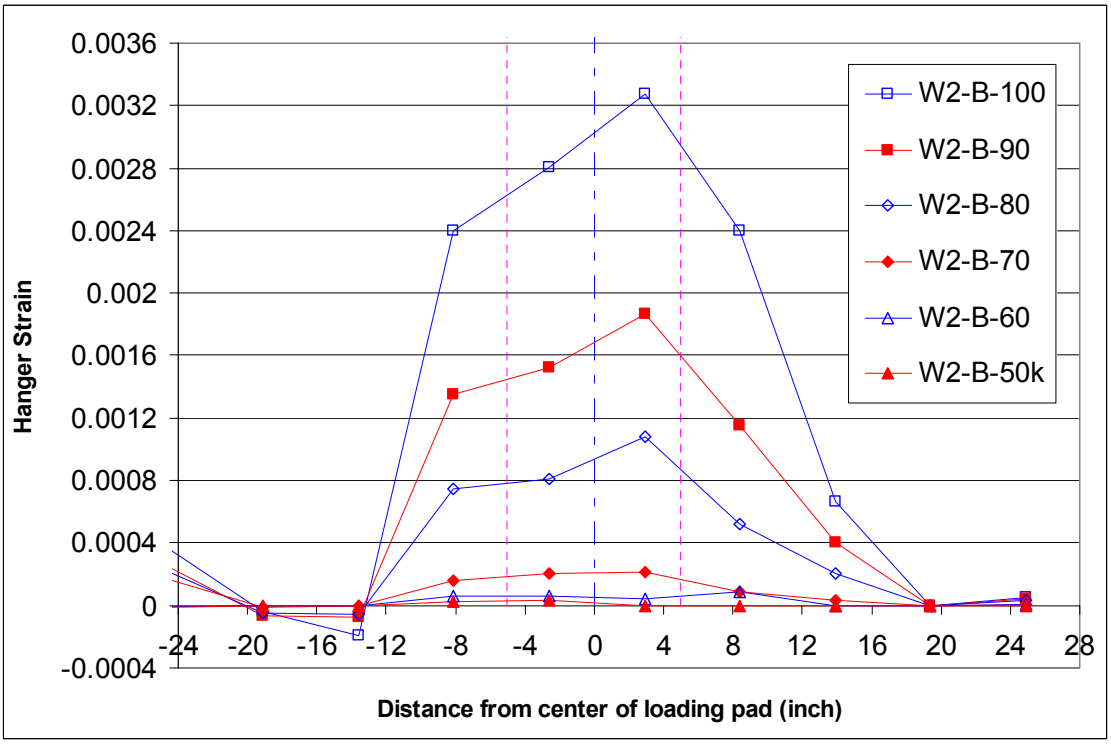

Fig. 4.3.2(c) Hanger strain variation along span (W2-B)

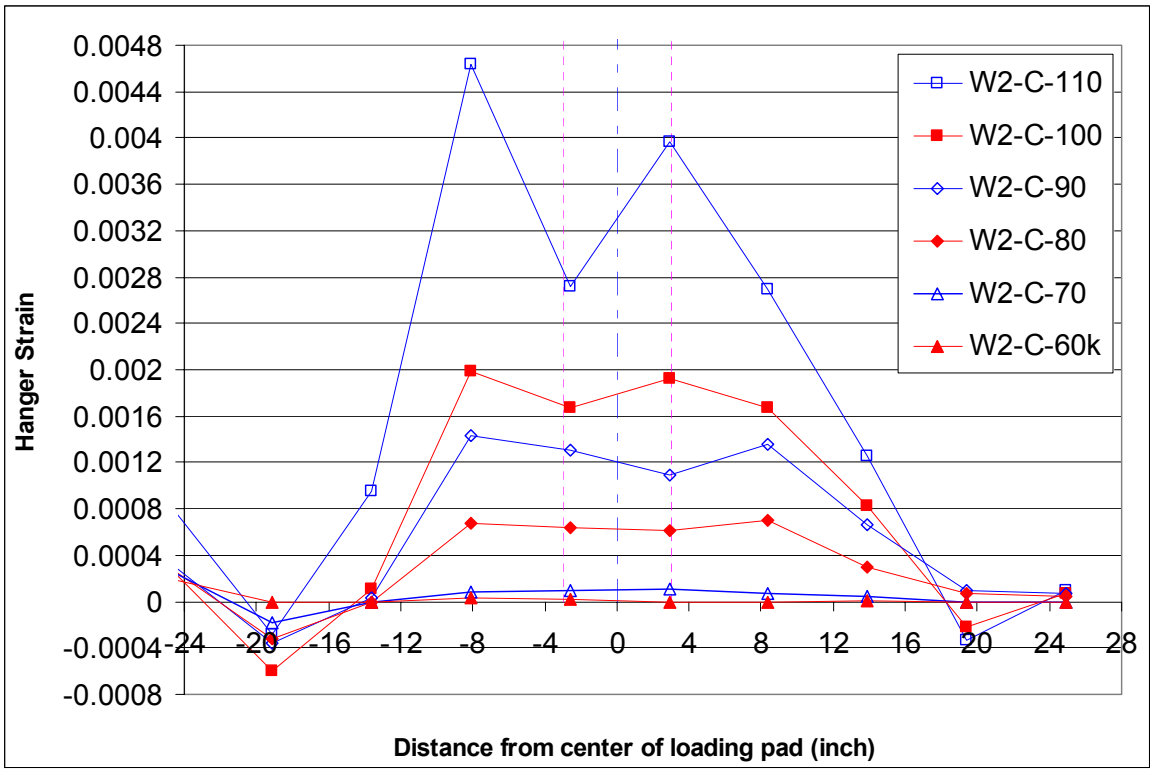

Fig. 4.3.2(d) Hanger strain variation along span (W2-C)

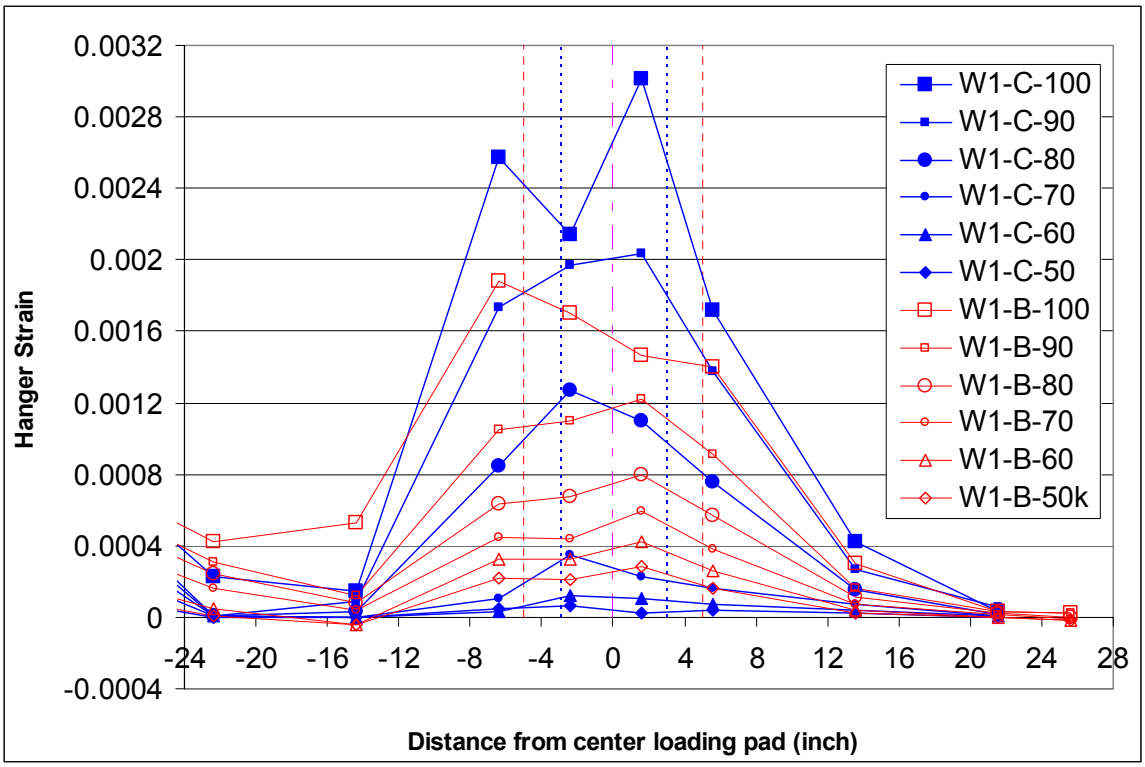

Fig. 4.3.2(e) Comparison of hanger strain variation between W1-B and W1-C

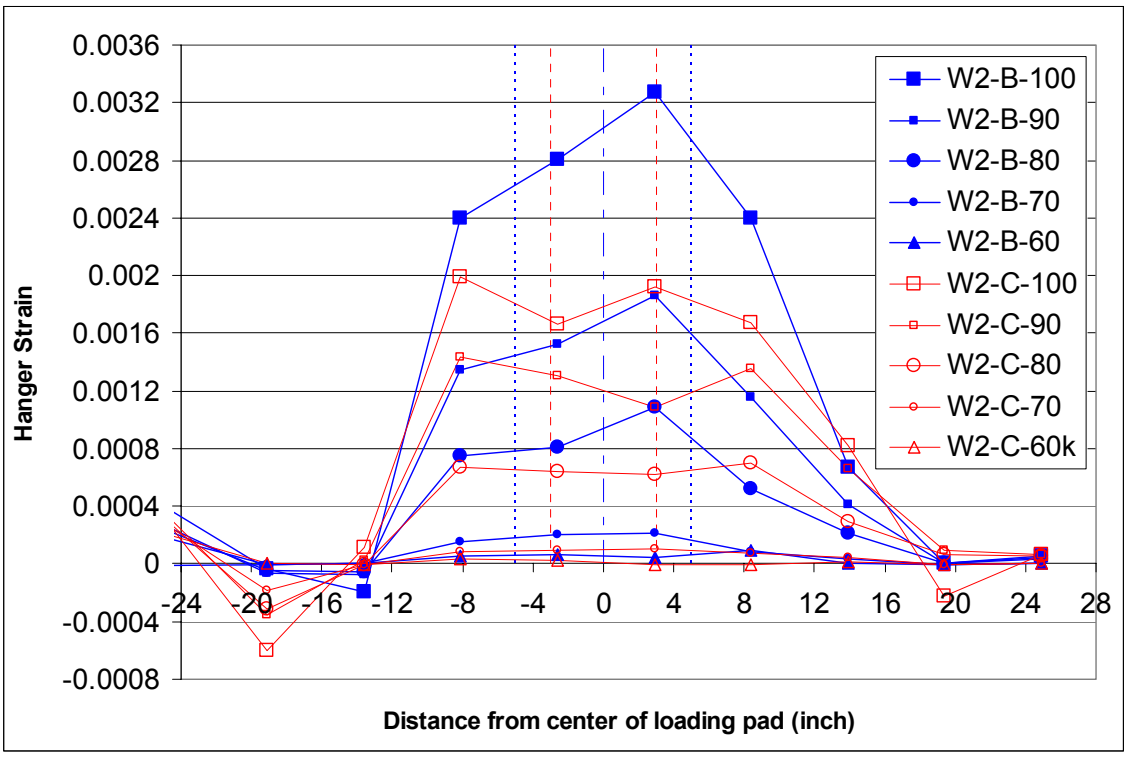

Fig. 4.3.2(f) Comparison of hanger strain variation between W2-B and W2-C

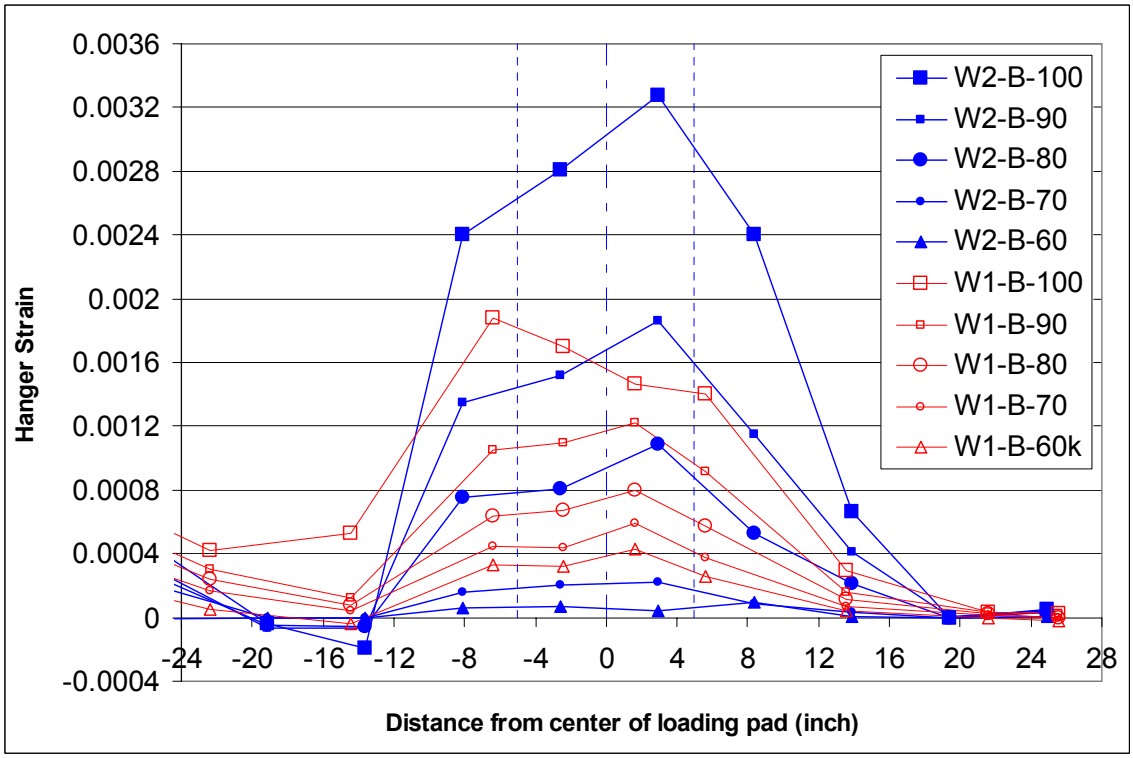

Fig. 4.3.2(g) Comparison of hanger strain variation between W1-B and W2-B

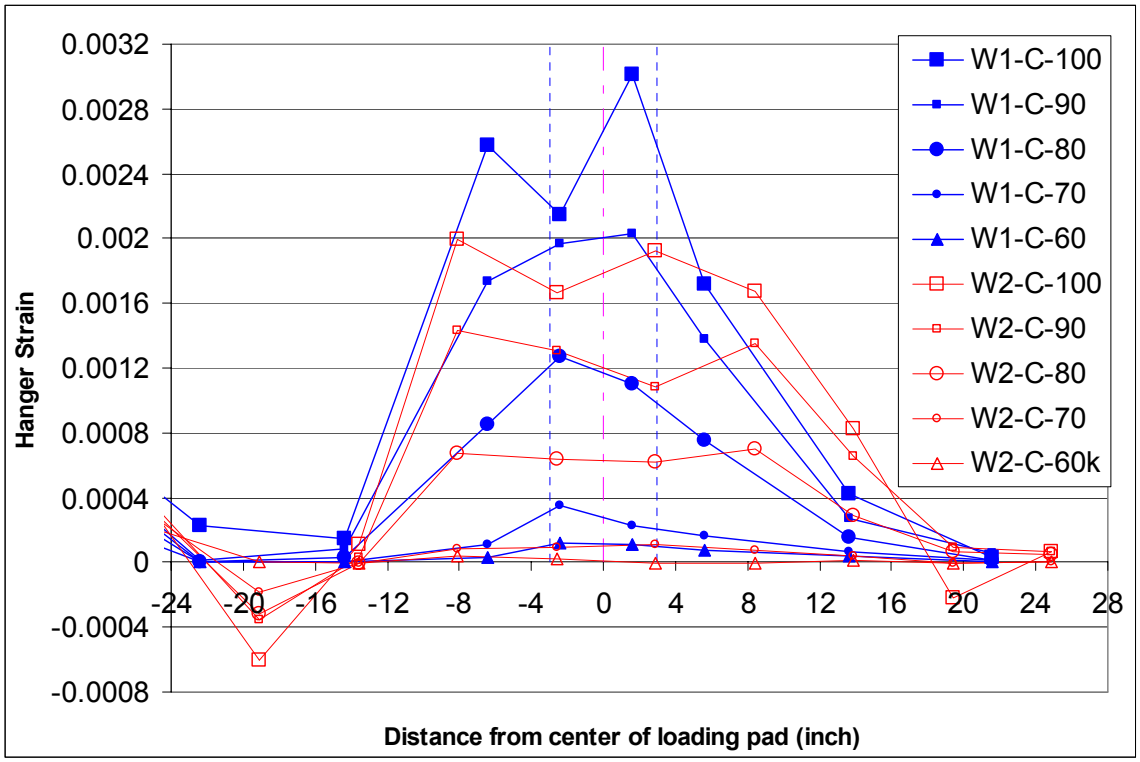

Fig. 4.3.2(h) Comparison of hanger strain variation between W1-C and W2-C

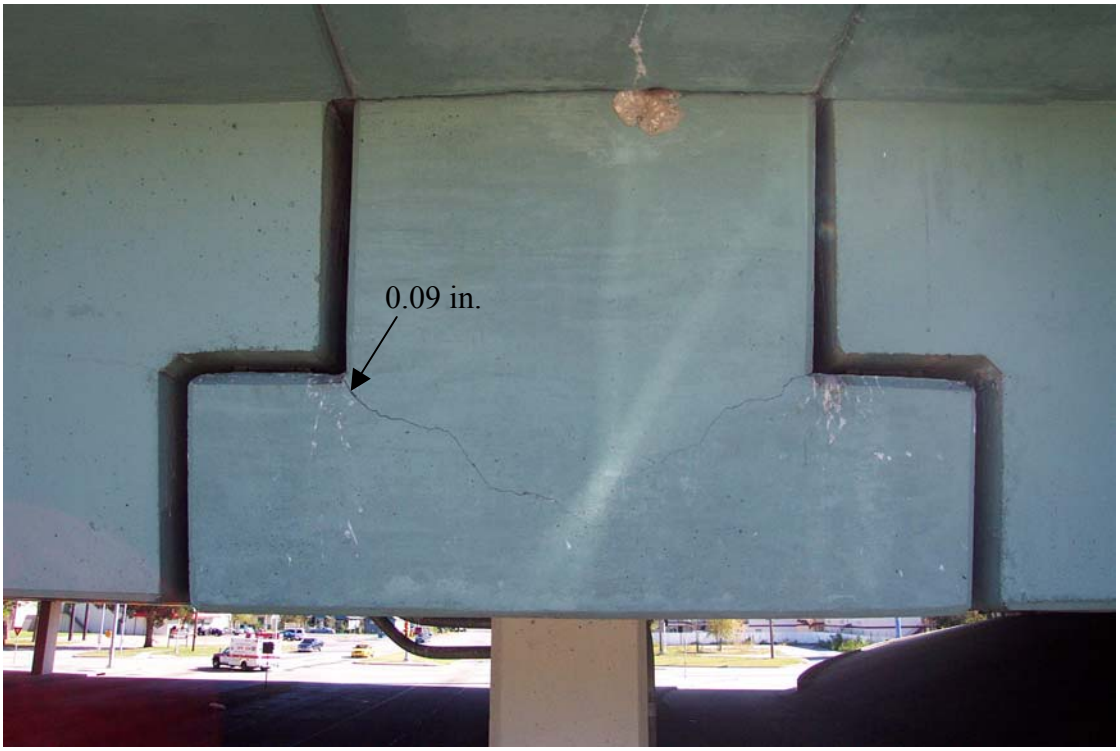

Fig. 4.4(a) Crack width at west end face of southwest inverted "T" bent cap at Laura Koppe Road

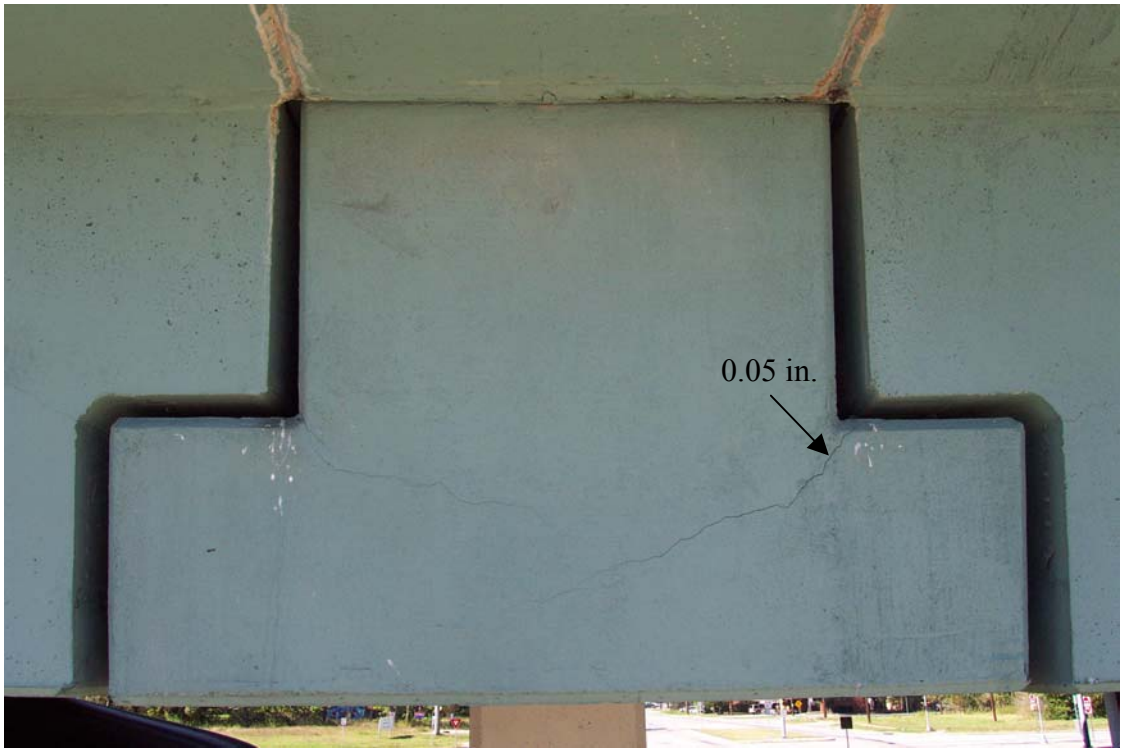

Fig. 4.4(b) Crack width at east end face of southeast inverted "T" bent cap at Laura Koppe Road

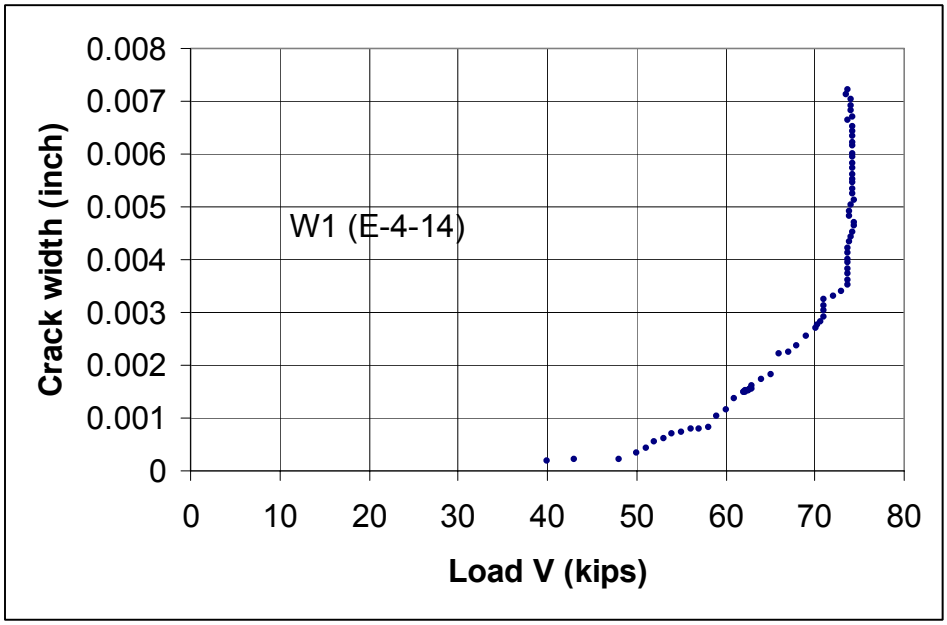

Fig. 5.1 Crack width open-up under constant load

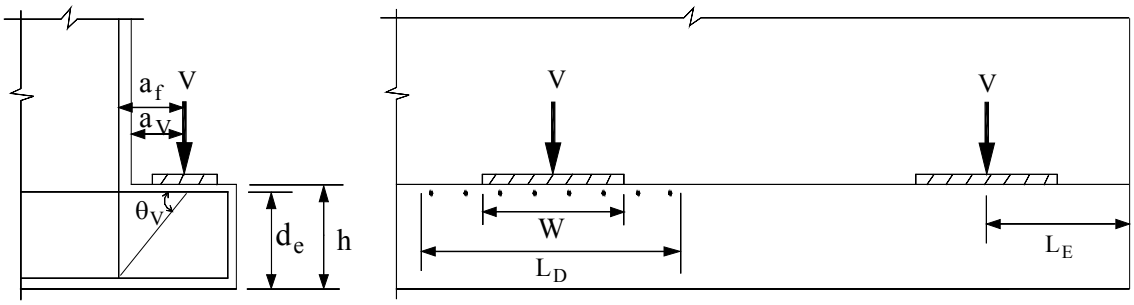

Fig. 5.2 Notation for inverted T-beam

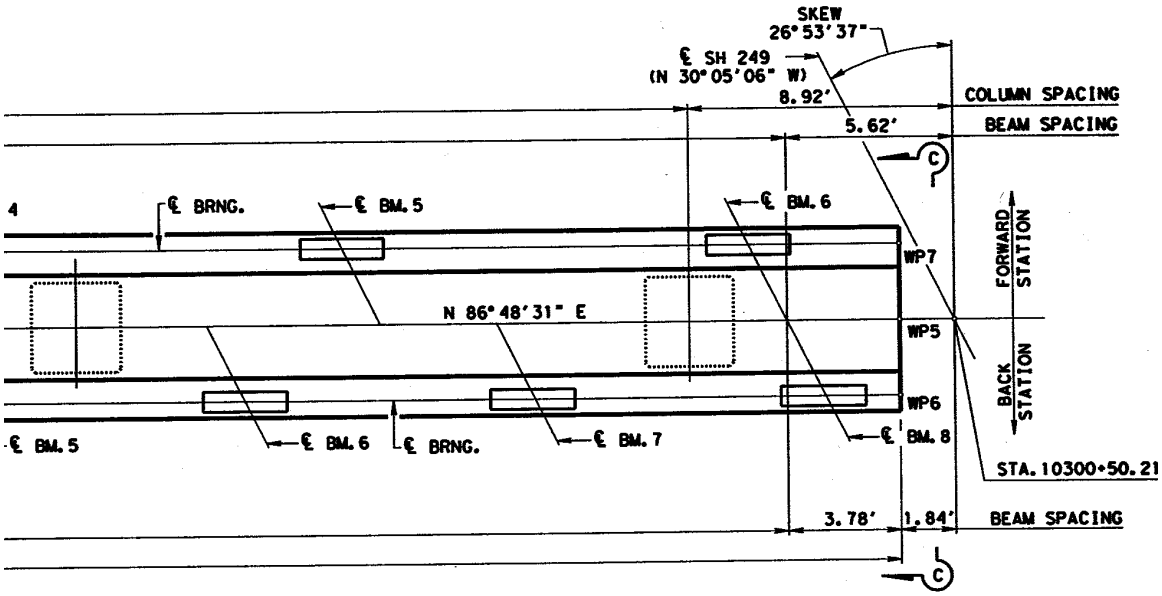

Fig. 6.1 Inverted T-beam in Spring Cypress Overpass

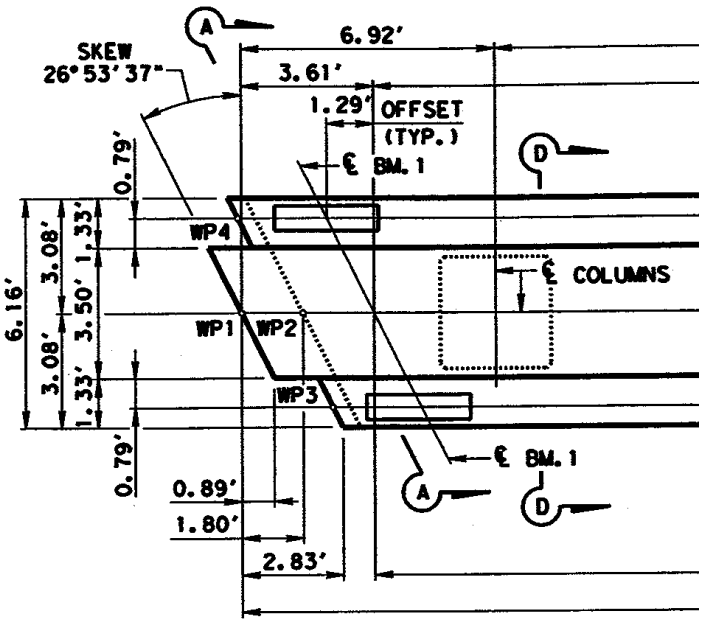

Fig. 6.2 Skewed end face in cantilever portion with inverted T-beam

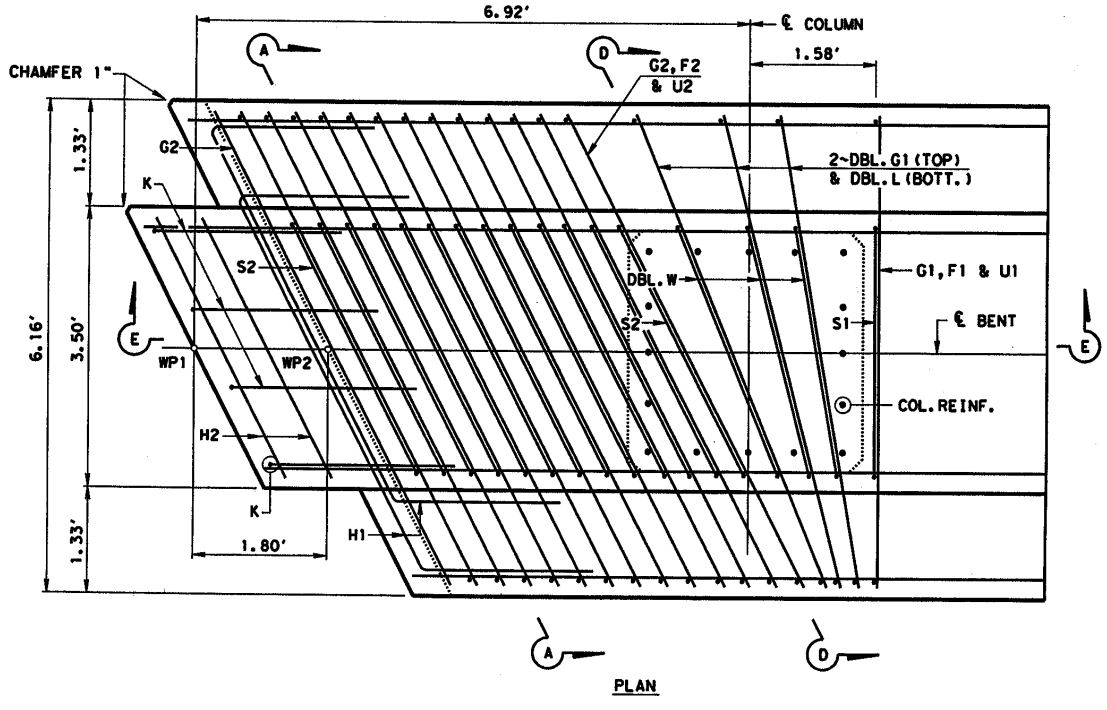

Fig. 6.3 Steel arrangement in cantilever portion with skewed end face

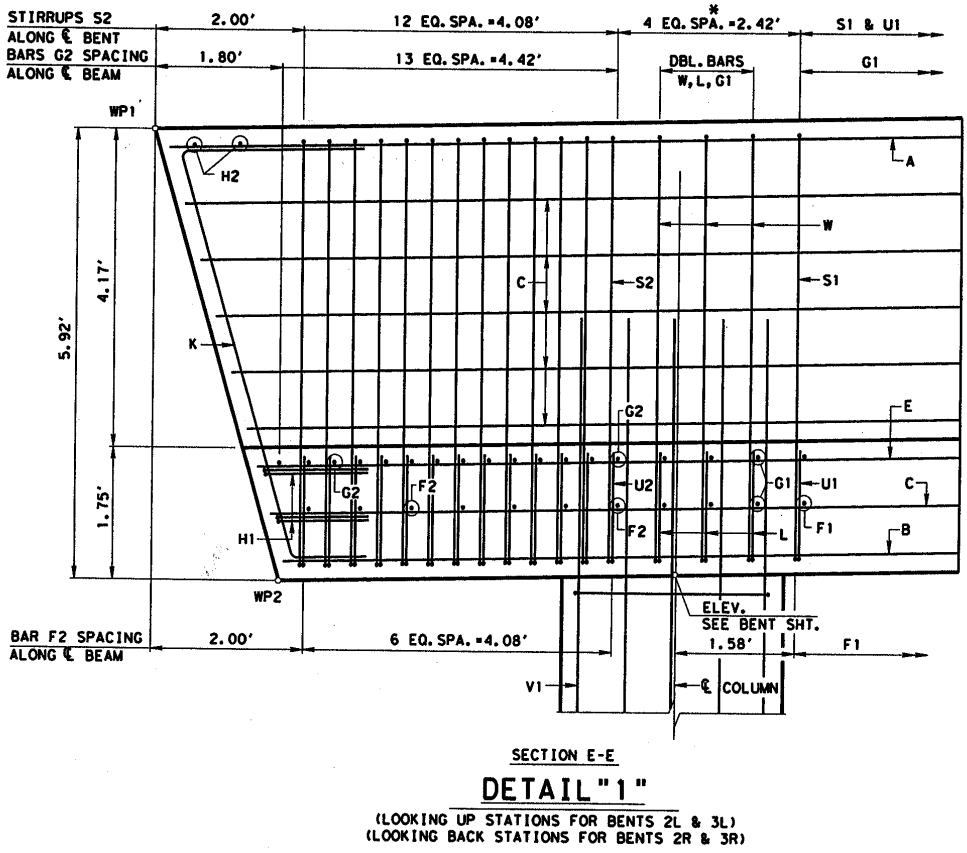

Fig. 6.4 Steel arrangement in cantilever portion with skewed end face

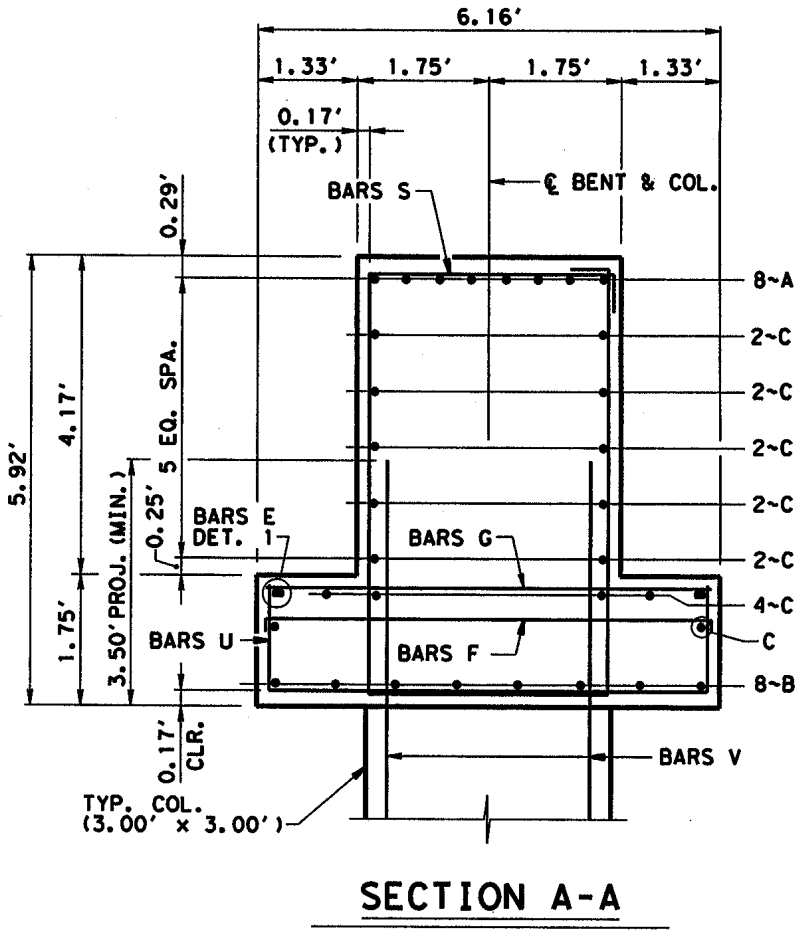

Fig. 6.5 A section parallel to skewed end face in cantilever portion (see section A-A in Fig 6.2)

Design Example 1 for Normal End

C-S-J: 0720-03-082

LOCATION: SH-249/Spring Cypress Overpass

Design by: TxDOT on 4/27/99

CALCULATED OUTPUT RESULTS			
Given V =	221	K	
Calculated $V_{0.006}$ =	135.5	K	
$V_{0.006}$ / V =	0.61		N.G. !

INPUT DATA

Design service load 'V' =	221	kips
Skew angle 'θ' =	0	deg
Clear concrete cover 'c' =	2	in
Ledge height 'h' =	21	in
Normal distance from load V to web edge 'a_V' =	9.5	in
Distance from load V to end face 'L_E' =	29.9	in
Hanger bar diameter 'd_{bH}' =	0.75	in
Hanger bar area 'A_{SH}' =	0.44	in^2
Flexural bar diameter 'd_{bF}' =	0.75	in
Flexural bar area 'A_{SF}' =	0.44	in^2
Diagonal bar area 'A_{SD}' =	0	in^2
Number of diagonal bar in distance L_E 'N' =	0	
Diagonal bar spacing 'S_D' (= hanger bar spacing) =	4.08	in
E_S =	29,000	ksi

TRIAL & ERROR TO FIND $V_{0.006}$

Assume $V_{0.006}$ = **135.5** kips

a_f = $(a_V + c)/\cos\theta + 0.5d_{bH}$ Distance from load V to center plane of hanger bar

= **11.9** in

θ_v = atan $[(h-2c-d_{bF})/a_f]$

= **0.94** rad **53.9** deg

A_{SD} = cross-sectional area of a diagonal steel bar at end face

= **0.00** in^2

A_{SH} = cross-sectional area of hanger reinforcement in a bar or a bundle

= **0.44** in^2

A_{SF}= cross-sectional area of flexural reinforcement in a bar or a bundle

= **0.44** in^2

B = distribution factor for diagonal bars

= $[A_{SD}/(A_{SH} + 0.5A_{SF} + A_{SD})][0.44NS_D/(1+L_E)]$

= **0.000**

ε_H = hanger bar strain

= $(1-B)V / (1.2E_SA_{SH})$

= **0.008849**

ε_F = flexural bar strain

= $(1-B)V \cot\theta_V / (1.2E_SA_{SF})$

= **0.006456**

ε_{HF} = diagonal crack strain calculated by hanger and flexural strains

= SQRT $(\varepsilon_H^2 + \varepsilon_F^2)$

= **0.010954**

L_{HF} = CASTM gauge length for calculated steel strains

= $9500\ \varepsilon_{HF} - 3.0$

= **101.06** in

w = predicted diagonal crack width *(aim for max of 0.006")*

= $2.6L_{HF}\varepsilon_{HF}/(1+0.7L_E)^2$ when w <= 0.006 in.

0.0060 in

Figure 6.6 Calculation example for normal end face of cantilever portion

Design Example 2 for Skewed End

C-S-J: 0720-03-082

LOCATION: SH-249/Spring Cypress Overpass

Design by: TxDOT on 4/27/99

CALCULATED OUTPUT RESULTS			
Given V =	215	K	
Calculated $V_{0.006}$ =	128.0	K	
$V_{0.006}$ / V =	0.60		N.G. !

INPUT DATA

Design service load 'V' =	215	kips
Skew angle 'θ' =	26.89	deg
Clear concrete cover 'c' =	2	in
Ledge height 'h' =	21	in
Normal distance from load V to web edge 'a_V' =	9.5	in
Distance from load V to end face 'L_E' =	29.3	in
Hanger bar diameter 'd_{bH}' =	0.75	in
Hanger bar area 'A_{SH}' =	0.44	in^2
Flexural bar diameter 'd_{bF}' =	0.75	in
Flexural bar area 'A_{SF}' =	0.44	in^2
Diagonal bar area 'A_{SD}' =	0	in^2
Number of diagonal bar in distance L_E 'N' =	0	
Diagonal bar spacing 'S_D' (= hanger bar spacing) =	4.08	in
E_S =	29,000	ksi

TRIAL & ERROR TO FIND $V_{0.006}$

Assume $V_{0.006}$ = 128 kips

a_f = $(a_V + c)/\cos\theta + 0.5d_{bH}$ Distance from load V to center plane of hanger bar

= 13.2 in

θ_v = atan $[(h-2c-d_{bF})/a_f]$

= **0.89** rad **50.8** deg

A_{SD} = cross-sectional area of a diagonal steel bar at end face

= 0.00 in^2

A_{SH} = cross-sectional area of hanger reinforcement in a bar or a bundle

= 0.44 in^2

A_{SF}= cross-sectional area of flexural reinforcement in a bar or a bundle

= 0.44 in^2

B = distribution factor for diagonal bars

= $[A_{SD}/(A_{SH} + 0.5A_{SF} + A_{SD})][0.44NS_D/(1+L_E)]$

= 0.000

ε_H = hanger bar strain

= $(1-B)V / (1.2E_SA_{SH})$

= 0.008359

ε_F = flexural bar strain

= $(1-B)V \cot\theta_V / (1.2E_SA_{SF})$

= 0.006814

ε_{HF} = diagonal crack strain calculated by hanger and flexural strains

= SQRT $(\varepsilon_H^2 + \varepsilon_F^2)$

= 0.010785

L_{HF} = CASTM gauge length for calculated steel strains

= $9500\ \varepsilon_{HF} - 3.0$

= 99.46 in

w = predicted diagonal crack width *(aim for max of 0.006")*

= $2.6L_{HF}\varepsilon_{HF}/(1+0.7L_E)^2$ when w <= 0.006 in.

0.0060 in

Figure 6.7 Calculation example for skewed end face of cantilever portion

Design Example 3 for Interior Portion

C-S-J: 0720-03-082

LOCATION: SH-249/Spring Cypress Overpass

Design by: TxDOT on 4/27/99

CALCULATION RESULTS			
Given V =	225	K	
Calculated $V_{0.013}$ =	174.0	K	
$V_{0.013}$ / V =	0.77		N.G. !

INPUTS

Design service load V =	225	kips
Clear concrete cover 'c' =	2	in
Ledge height 'h' =	21	in
Distance from load V to web edge 'a_V' =	9.5	in
Loading pad width 'W' =	34.0	in
Hanger bar diameter 'd_{bH}' =	0.75	in
Hanger bar area 'A_{SH}' =	0.44	in^2
Flexural bar diameter 'd_{bF}' =	0.75	in
Flexural bar area 'A_{SF}' =	0.44	in^2
Hanger Bar Spacing 'S_H'	5	in
Diagonal bar area 'A_{SD}' =	0	in^2
Diagonal bar spacing 'S_D' (same as hanger bar spacing) =	5	in
E_S =	29,000	ksi

TRIAL & ERROR TO FIND $V_{0.013}$

Assume $V_{0.013}$ = 174 kips

a_f = $(a_V + c) + 0.5d_{bH}$ Distance from load V to center plane of hanger bar

= 11.9 in

θ_v = atan $[(h-2c-d_{bF})/a_f]$

= **0.94** rad

L_D = **$W+0.9d_f$**

52.63 in

A_{SD} = total cross-sectional area of diagonal reinforcement in L_D

= 0.00 in^2

A_{SH} = total cross-sectional area of hanger reinforcement in L_D

= 4.63 in^2

A_{SF}= total cross-sectional area of flexural reinforcement in L_D

= 4.63 in^2

B = distribution factor for diagonal bars

= $A_{SD}/(A_{SH} + 0.5A_{SF} + A_{SD})$

= 0.000

ε_H = hanger strain

= $(1-B)V / (1.2E_SA_{SH})$

= 0.001080

ε_F = flexural strain

= $(1-B)V \cot \theta_V / (1.2E_SA_{SF})$

= 0.000788

ε_{HF} = diagonal crack strain calculated by hanger and flexural strains

= SQRT $(\varepsilon_H^2 + \varepsilon_F^2)$

= 0.001336

L_{HF} = CASTM gauge length for calculated steel strains

= $9500\ \varepsilon_{HF} - 3.0$

= 9.70 in

w = predicted diagonal crack width *(aim for max of 0.013")*

= $L_{HF}\varepsilon_{HF}$

0.0130 in

Figure 6.8 Calculation example for interior portion of inverted T beam

Appendix A

Simplification of Steel Tie Stiffness

Equation (2.1) and (3.4) for crack width prediction have been simplified by taking the stiffness EI of a steel tie with concrete cover to be $1.2\,E_sA_s$. The accuracy of this simplification can be demonstrated by the following derivation.

$$EA = E_sA_s + E_cA_c$$

$$= E_sA_s(1 + \frac{E_cA_c}{E_sA_s})$$

$$= E_sA_s(1 + \frac{1866\sqrt{f_c'}A_c}{29000000A_s})$$

Based on a minimum net cover of 2-inch for No. 6 and larger bar, required by the ACI code,

$$A_c = \pi(2 + 0.5d_b)^2$$

Where d_b = steel bar diameter (inch)

Therefore

$$EA = E_sA_s\left[1 + \frac{1866\sqrt{f_c'}\pi(2 + 0.5d_b)^2}{29000000\pi\frac{d_b^2}{4}}\right]$$

and $$EA = \eta E_sA_s$$

The coefficient η is calculated in Table A. Table A shows that η can be approximated by a constant 1.2 for steel bars equal to or less than No. 6.

Table A Parameter η

Steel Bar	f'_c (psi)	η	Average η
No. 5	4000	1.22	1.2
No. 5	5000	1.25	
No. 6	4000	1.16	
No. 6	5000	1.18	
No. 7	4000	1.13	1.12
No. 7	5000	1.14	
No. 8	4000	1.10	
No. 8	5000	1.11	

Appendix B

Direct Calculation of $V_{0.006}$

There are two ways to calculate $V_{0.006}$. The first way is to use trial-and-error method (spreadsheet) to solve Eq. (4.6) as shown in Fig. 6.6. The second way is to solve Eq. (4.6) directly, resulting in:

$$V_{0.006} = \frac{1.83\left(3+\sqrt{9+87.4(1+0.7L_E)^2}\right)}{(1-B)\sqrt{\frac{1}{A_{SH}{}^2}+\frac{1}{(A_{SF}\tan\theta_V)^2}}}$$

The above equation can be simplified into an expression as follows:

$$V_{0.006} = \frac{(12L_E+22)A_{SH}}{(1-B)}\left(1-\frac{0.45A_{SH}a_V}{A_{SF}h\cos\theta}\right)$$

where:

B = distribution factor for diagonal bars $= \frac{A_{SD}}{A_{SH}+0.5A_{SF}+A_{SD}}\left(\frac{0.44NS_D}{1+L_E}\right)$

V = applied service load at the most exterior loading pad (kips)

$V_{0.006}$ = applied service load at the most exterior loading pad when crack width reaches 0.006 in. (kips)

θ = skew angle

θ_V = angle between flexural steel bars and the diagonal strut at the point of load V

a_V = normal distance from load V to web edge, inch

h = ledge height, inch

A_{SD} = cross-sectional area of a diagonal steel bar at edge of inverted 'T' bent cap ($in.^2$)

A_{SH} = cross-sectional area of a hangar steel bar at edge of inverted 'T' bent cap ($in.^2$)

A_{SF} = cross-sectional area of a flexural steel bar at edge of inverted 'T' bent cap ($in.^2$)

L_E = the distance from end face to the load V applied on the most exterior bearing, inch

N = number of diagonal bars from the end face to the center of first bearing

S_D = center-to-center spacing of diagonal bars, same as spacing of hangar bars, inch.

Appendix C

Redesign Examples

Design Example 1 for Normal End

C-S-J: 0720-03-082

LOCATION: SH-249/Spring Cypress Overpass

Design by: TxDOT on 4/27/99

Redesign by adding diagonal bars

CALCULATED OUTPUT RESULTS			
Given V =	221	K	
Calculated $V_{0.006}$ =	162.0	K	
$V_{0.006}$ / V =	0.73		N.G. !

INPUT DATA

Design service load 'V' =	**221**	kips
Skew angle 'θ' =	**0**	deg
Clear concrete cover 'c' =	**2**	in
Ledge height 'h' =	**21**	in
Normal distance from load V to web edge 'a_V' =	**9.5**	in
Distance from load V to end face 'L_E' =	**29.9**	in
Hanger bar diameter 'd_{bH}' =	**0.75**	in
Hanger bar area 'A_{SH}' =	**0.44**	in^2
Flexural bar diameter 'd_{bF}' =	**0.75**	in
Flexural bar area 'A_{SF}' =	**0.44**	in^2
Diagonal bar area 'A_{SD}' =	**0.44**	in^2
Number of diagonal bar in distance L_E 'N' =	**7**	
Diagonal bar spacing 'S_D' (= hanger bar spacing) =	**4.08**	in
E_S =	**29,000**	ksi

TRIAL & ERROR TO FIND $V_{0.006}$

Assume $V_{0.006}$ = **162** kips

a_f = $(a_V + c)/\cos\theta + 0.5d_{bH}$ Distance from load V to center plane of hanger bar

= **11.9** in

θ_v = atan $[(h-2c-d_{bF})/a_f]$

= **0.94** rad **53.9** deg

A_{SD} = cross-sectional area of a diagonal steel bar at end face

= **0.44** in^2

A_{SH} = cross-sectional area of hanger reinforcement in a bar or a bundle

= **0.44** in^2

A_{SF}= cross-sectional area of flexural reinforcement in a bar or a bundle

= **0.44** in^2

B = distribution factor for diagonal bars

= $[A_{SD}/(A_{SH} + 0.5A_{SF} + A_{SD})][0.44NS_D/(1+L_E)]$

= **0.163**

ε_H = hanger bar strain

= $(1-B)V / (1.2E_SA_{SH})$

= **0.008859**

ε_F = flexural bar strain

= $(1-B)V \cot\theta_V / (1.2E_SA_{SF})$

= **0.006463**

ε_{HF} = diagonal crack strain calculated by hanger and flexural strains

= SQRT $(\varepsilon_H^2 + \varepsilon_F^2)$

= **0.010966**

L_{HF} = CASTM gauge length for calculated steel strains

= $9500\ \varepsilon_{HF} - 3.0$

= **101.18** in

w = predicted diagonal crack width *(aim for max of 0.006")*

= $2.6L_{HF}\varepsilon_{HF}/(1+0.7L_E)^2$ when w <= 0.006 in.

0.0060 in

Design Example 1 for Normal End

C-S-J: 0720-03-082

LOCATION: SH-249/Spring Cypress Overpass

Design by: TxDOT on 4/27/99

Redesign by increasing hanger and flexural bar

CALCULATED OUTPUT RESULTS			
Given V =	221	K	
Calculated $V_{0.006}$ =	221.0	K	
$V_{0.006}$ / V =	1.00		O.K. !

INPUT DATA

Design service load 'V' =	**221**	kips
Skew angle 'θ' =	**0**	deg
Clear concrete cover 'c' =	**2**	in
Ledge height 'h' =	**21**	in
Normal distance from load V to web edge 'a_V' =	**9.5**	in
Distance from load V to end face 'L_E' =	**29.9**	in
Hanger bar diameter 'd_{bH}' =	**0.75**	in
Hanger bar area 'A_{SH}' =	**0.715**	in^2
Flexural bar diameter 'd_{bF}' =	**0.75**	in
Flexural bar area 'A_{SF}' =	**0.715**	in^2
Diagonal bar area 'A_{SD}' =	**0**	in^2
Number of diagonal bar in distance L_E 'N' =	**0**	
Diagonal bar spacing 'S_D' (= hanger bar spacing) =	**4.08**	in
E_S =	**29,000**	ksi

TRIAL & ERROR TO FIND $V_{0.006}$

Assume $V_{0.006}$ = **221** kips

a_f = $(a_V + c)/\cos\theta + 0.5d_{bH}$ Distance from load V to center plane of hanger bar

= **11.9** in

θ_v = atan $[(h-2c-d_{bF})/a_f]$

= **0.94** rad **53.9** deg

A_{SD} = cross-sectional area of a diagonal steel bar at end face

= **0.00** in^2

A_{SH} = cross-sectional area of hanger reinforcement in a bar or a bundle

= **0.72** in^2

A_{SF} = cross-sectional area of flexural reinforcement in a bar or a bundle

= **0.72** in^2

B = distribution factor for diagonal bars

= $[A_{SD}/(A_{SH} + 0.5A_{SF} + A_{SD})][0.44NS_D/(1+L_E)]$

= **0.000**

ε_H = hanger bar strain

= $(1-B)V / (1.2E_SA_{SH})$

= **0.008882**

ε_F = flexural bar strain

= $(1-B)V \cot\theta_V / (1.2E_SA_{SF})$

= **0.006480**

ε_{HF} = diagonal crack strain calculated by hanger and flexural strains

= SQRT $(\varepsilon_H^2 + \varepsilon_F^2)$

= **0.010994**

L_{HF} = CASTM gauge length for calculated steel strains

= $9500\ \varepsilon_{HF} - 3.0$

= **101.45** in

w = predicted diagonal crack width *(aim for max of 0.006")*

= $2.6L_{HF}\varepsilon_{HF}/(1+0.7L_E)^2$ when w <= 0.006 in.

0.0060 in

Design Example 3 for Interior Portion

C-S-J: 0720-03-082

LOCATION: SH-249/Spring Cypress Overpass

Design by: TxDOT on 4/27/99

Redesign by reducing hanger bar spacing

CALCULATION RESULTS			
Given V =	225	K	
Calculated $V_{0.013}$ =	225.0	K	
$V_{0.013}$ / V =	1.00		O.K. !

INPUTS

Design service load V =	**225**	kips
Clear concrete cover 'c' =	**2**	in
Ledge height 'h' =	**21**	in
Distance from load V to web edge 'a_V' =	**9.5**	in
Loading pad width 'W' =	**34.0**	in
Hanger bar diameter 'd_{bH}' =	**0.75**	in
Hanger bar area 'A_{SH}' =	**0.44**	in^2
Flexural bar diameter 'd_{bF}' =	**0.75**	in
Flexural bar area 'A_{SF}' =	**0.44**	in^2
Hanger Bar Spacing 'S_H'	**3.87**	in
Diagonal bar area 'A_{SD}' =	**0**	in^2
Diagonal bar spacing 'S_D' (same as hanger bar spacing) =	**3.87**	in
E_S =	**29,000**	ksi

TRIAL & ERROR TO FIND $V_{0.013}$

Assume $V_{0.013}$ = **225** kips

a_f = $(a_V + c) + 0.5d_{bH}$ Distance from load V to center plane of hanger bar

= **11.9** in

θ_v = atan $[(h-2c-d_{bF})/a_f]$

= **0.94** rad

L_D = W+0.9d_f

52.63 in

A_{SD} = total cross-sectional area of diagonal reinforcement in L_D

= **0.00** in^2

A_{SH} = total cross-sectional area of hanger reinforcement in L_D

= **5.98** in^2

A_{SF}= total cross-sectional area of flexural reinforcement in L_D

= **5.98** in^2

B = distribution factor for diagonal bars

= $A_{SD}/(A_{SH} + 0.5A_{SF} + A_{SD})$

= **0.000**

ε_H = hanger strain

= $(1-B)V / (1.2E_SA_{SH})$

= **0.001081**

ε_F = flexural strain

= $(1-B)V \cot \theta_V / (1.2E_SA_{SF})$

= **0.000788**

ε_{HF} = diagonal crack strain calculated by hanger and flexural strains

= SQRT $(\varepsilon_H^2 + \varepsilon_F^2)$

= **0.001338**

L_{HF} = CASTM gauge length for calculated steel strains

= 9500 ε_{HF} - 3.0

= **9.71** in

w = predicted diagonal crack width *(aim for max of 0.013")*

= $L_{HF}\varepsilon_{HF}$

0.0130 in

Design Example 3 for Interior Portion

C-S-J: 0720-03-082

LOCATION: SH-249/Spring Cypress Overpass

Design by: TxDOT on 4/27/99

Redesign by adding diagonal bars

CALCULATION RESULTS			
Given V =	225	K	
Calculated $V_{0.013}$ =	225.0	K	
$V_{0.013}$ / V =	1.00		O.K. !

INPUTS

Design service load V =	**225**	kips
Clear concrete cover 'c' =	**2**	in
Ledge height 'h' =	**21**	in
Distance from load V to web edge 'a_V' =	**9.5**	in
Loading pad width 'W' =	**34.0**	in
Hanger bar diameter 'd_{bH}' =	**0.75**	in
Hanger bar area 'A_{SH}' =	**0.44**	in^2
Flexural bar diameter 'd_{bF}' =	**0.75**	in
Flexural bar area 'A_{SF}' =	**0.44**	in^2
Hanger Bar Spacing 'S_H'	**5**	in
Diagonal bar area 'A_{SD}' =	**0.191**	in^2
Diagonal bar spacing 'S_D' (same as hanger bar spacing) =	**5**	in
E_S =	**29,000**	ksi

TRIAL & ERROR TO FIND $V_{0.013}$

Assume $V_{0.013}$ = **225** kips

a_f = $(a_V + c) + 0.5d_{bH}$ Distance from load V to center plane of hanger bar

= **11.9** in

θ_V = atan $[(h-2c-d_{bF})/a_f]$

= **0.94** rad

L_D = $W+0.9d_f$

52.63 in

A_{SD} = total cross-sectional area of diagonal reinforcement in L_D

= **2.01** in^2

A_{SH} = total cross-sectional area of hanger reinforcement in L_D

= **4.63** in^2

A_{SF} = total cross-sectional area of flexural reinforcement in L_D

= **4.63** in^2

B = distribution factor for diagonal bars

= $A_{SD}/(A_{SH} + 0.5A_{SF} + A_{SD})$

= **0.224**

ε_H = hanger strain

= $(1-B)V / (1.2E_SA_{SH})$

= **0.001083**

ε_F = flexural strain

= $(1-B)V \cot \theta_V / (1.2E_SA_{SF})$

= **0.000790**

ε_{HF} = diagonal crack strain calculated by hanger and flexural strains

= SQRT $(\varepsilon_H^2 + \varepsilon_F^2)$

= **0.001340**

L_{HF} = CASTM gauge length for calculated steel strains

= $9500\ \varepsilon_{HF} - 3.0$

= **9.73** in

w = predicted diagonal crack width *(aim for max of 0.013")*

= $L_{HF}\varepsilon_{HF}$

0.0130 in